Interactive comment on "Measurement report: Quantifying source contribution and radiative forcing of fossil fuel and biomass burning black carbon aerosol in the southeastern margin of Tibetan Plateau" by Huikun Liu et al.

Anonymous Referee #1

General comments: In this manuscript, the sources of BC aerosols over the Tibetan Plateau and their radiative effects were investigated. BC aerosols were distinguished into fossil fuel combustion source and biomass burning source. Regional transport of source-specific BC was further explored by models. On this basis, the radiative effects caused by BC from different sources were evaluated. Overall, the manuscript is well structured, the methods are technically sound, and the main findings presented seem to be reasonable and be of general interests to the Tibetan Plateau ecosystem and climate stability study. I think the topic fits within the scope of ACP. I would recommend acceptance of this manuscript for publication pending the following revisions:

Response: We sincerely thank the reviewer for the comments and suggestions, and we have revised the relevant text and content. Below are point-to-point responses, and the modifications to the manuscript are marked.

Specific comments:

1.Please spend time picking through the manuscript and check for spelling and grammatical errors, especially the tense, prepositions and articles. For example, 'BC on the TP' should be replaced with 'BC over the TP', 'transport to TP' should be replaced with 'transport to the TP'

Response: We have taken the suggestion to heart and have corrected the relevant mistakes as shown below. Also, the paper has been polished by a native English speaker.

> "Therefore, quantitative information on the contributions of different sources of BC over the TP is lacking, but it is critically needed for a better understanding the influence of anthropogenic emissions on its environment and climate."

> "Nonetheless, these studies have been helpful for understanding the sources of BC over the TP."

2.Section 1, this part should introduce the research background and significance, current status, concealed problems, as well as research mentality and content of this study. Please highlight the innovation and importance from another angle and reduce describing the deficiencies of previous research appropriately.

Response: We have re-written the introduction to include more background material, to clarify the research focus, to explain why we were interested in study area and why we chose the methods we did. The revised introduction now reads:

"The Tibetan Plateau (TP) is an important regulator of climate change in the northern hemisphere, and it plays crucial roles in the functions of global ecosystems and climate stability (Liu et al., 2019b; Liu et al., 2020a). The TP is covered by one of the largest ice masses on Earth, and it has been called the water tower of Asia (Liu et al., 2020b). The glaciers on the TP are facing rapid retreat, however, and if unchecked, that could result in adverse effects on Asian hydrological cycle and the Asian monsoon (Luo et al., 2020; Hua et al., 2019). In spring, the glaciers on the TP begin to melt as part of the natural hydrological cycle, but the increasing quantities of black carbon (BC) aerosol transported to the TP has accelerated this process (Bond et al., 2013) by causing a warming effect in atmosphere over the TP and enhancing the absorption of radiation on the surface of the glaciers (Ming et al., 2009).

The southern part of the TP is bounded by South Asia where air pollution often is severe (Chan et al. 2017). Several studies have shown that pollutants (including BC) from South Asia can be transported to the south of the TP along mountain-valleys, especially during the pre-monsoon (March–May) when southwestly winds prevail (e.g., Cao et al., 2010; Xia et al., 2011 Zhu et al., 2017; Niu et al. 2017). For example, Xia et al., (2011) analyzed satellite data and air mass trajectories and found that the TP, particularly the southern TP, was affected by pollutants carried by southwesterly winds from nearby regions in South Asia. In addition, numerous studies have shown that the high bulk BC mass loadings and the associated regional influences on the TP are related to transport from South Asia (Liu et al., 2015; Han et al., 2020; Cong et al., 2015; Wang et al., 2015). Nonetheless, assessments of regional transport of bulk BC aerosol have not fully revealed the impacts of different BC emission sources because the optical properties and radiative effects of BC not only can vary among sources in complex ways but also can be affected by aging during transport (Tian et al., 2019; Zhang et al., 2019). Therefore, quantitative information on the contributions of different sources of BC over the TP is lacking, but it is critically needed for a better understanding the influence of anthropogenic emissions on its environment and climate.

Several studies have assessed the contributions of different BC sources through model simulations or isotopic methods. For example, Zhang et al. (2015) investigated BC sources for different parts of the TP by using a chemical transport model and a source tagging approach, and they found that the contributions of BC sources varied among regions and with the seasons. Li et al., (2016) used filter

sampling and carbon isotopes ($\Delta^{14}C$ and $\delta^{13}C$) to determine the BC from fossil fuels and biomass burning in several areas of the TP. A major disadvantage of filter-based measurements is they are constrained by low time resolution, and this makes it challenging to capture the detailed evolution of pollution events. On the other hand, the accuracy of model simulations is dependent on many factors, including uncertainties associated with initial particle parameters, aging processes, the accuracy of emission inventory, meteorological fields over the complex terrain, and the modules for chemistry and planetary boundary layer (PBL) dynamics, etc. (Koch et al., 2009; Madala et al., 2014; Vignati et al., 2010). Nonetheless, these studies have been helpful for understanding the sources of BC over the TP.

To make up for the deficiencies of filter-based analysis, BC source apportionments based on high-time resolution online data has been conducted in many locations but for the TP are limited. An 'aethalometer model' based on multi-wavelength absorption data is one of efficient approaches for distinguishing between BC from fossil fuel and biomass burning sources (Sandradewi et. al., 2008). Although it has been widely used elsewhere, this approach has not been applied to the TP. The accuracy of the 'aethalometer model' relies on the input parameters, including the Ångström exponents (AAE) and BC mass absorption cross-sections (MAC_{BC}) of different sources (Zotter et al., 2017). Limited information on site specific AAEs and MAC_{BC}s, lead most studies to rely on values taken from measurements made in other locations (e.g., Healy et al., 2017; Zhu et al., 2017). This results in unquantified uncertainties because the AAEs and MAC_{BC}s vary with specific fuel subtypes and combustion conditions (Wang et al., 2018; Tian et al., 2019). Therefore, site-dependent AAE and MAC_{BC} are essential for improving the reliability of BC source apportionment by the 'aethalometer model'.

In this study, field measurements of BC were taken on the southeastern margin of the TP during the pre-monsoon. This region connects the high altitude TP with the low altitude Yungui Plateau and forms a transport channel for pollutants from Southeast Asia (Wang et al., 2019a), and it is an ideal region for investigating the impact of pollutant transport to the southeastern TP. A receptor model that combined multi-wavelength absorption with aerosol species concentrations was used to retrieve site-dependent AAEs and MAC_{BC}s. This was done to improve the 'aethalometer model' with the goal of obtaining a more accurate BC source apportionment. The primary objectives of this study were to (1) quantify the mass concentrations of BC from fossil fuel and biomass burning sources; (2) determine the impact of regional transport on source-specific BC; and (3) assess the radiative effects caused by BC from different sources. This study provides insights into the BC sources on southeastern TP and an assessment of their radiative effects during the pre-monsoon."

3.Please try to avoid expressions like 'our study', which seems not be objective. Technical corrections: 1.P1, Line 24, 'reveal' should be changed to 'revealed'.

Response: We have changed all "our study" in the manuscript into "this study". The verbal tenses have been correct in the following sentence:

> "The potential source contribution function indicated that $BC_{biomass}$ was transported to the site from northeastern India and northern Burma."

2.P1, Line 26, add 'which' before 'can explain'.

Response: We have changed the sentence to

> "The Weather Research and Forecasting model coupled with chemistry (WRF-Chem) model indicated that 40% of the $BC_{biomass}$ originated from Southeast Asia"

3.P2, Line 1, delete 'and' before 'heating rates of'.

Response: We have changed this sentence to

> "The DRE of $BC_{biomass}$ and BC_{fossil} produced heating rates of 0.07 ± 0.05 and 0.06 ± 0.02 K day^{-1}, respectively."

4.P2, Line 1, 'The glaciers on the TP recently shows are rapidly retreating' should be revised.

Response: We have corrected this to

> "The glaciers on the TP are facing rapid retreat, however, and if unchecked, that could result in adverse effects on Asian hydrological cycle and the Asian monsoon (Luo et al., 2020; Hua et al., 2019)."

5.P2, Line 4-8, Please cite these literatures, doi:10.1093/nsr/nwz191, doi.org/10.1016/j.atmosenv.2020.117583, doi: 10.1016/j.atmosenv.2019.04.001.

Response: We cite those papers in the revised version.

> "The Tibetan Plateau (TP) is an important regulator of climate change in the northern hemisphere, and it plays crucial roles in the functions of global ecosystems and climate stability (Liu et al., 2019b; Liu et al., 2020a). The TP is covered by one of the largest ice masses on Earth, and it has been called the water tower of Asia (Liu et al., 2020b)."

6.P2, Line 8-10, Please cite these literatures, doi.org/10.3390/rs12020231, doi:10.1002/joc.6430.

Response: We now cited these references in the revised version.

> "The glaciers on the TP are facing rapid retreat, however, and if unchecked, that could result in adverse effects on Asian hydrological cycle and the Asian monsoon (Luo et al., 2020; Hua et al., 2019)."

7.P2, Line 16, 'the atmospheric BC studies on the TP' should be changed to 'studies on the TP atmospheric BC'.

Response: We have revised the sentence

> "In addition, numerous studies have shown that the high bulk BC mass loadings and the associated regional influences on the TP are related to transport from South Asia (Liu et al., 2015; Han et al., 2020; Cong et al., 2015; Wang et al., 2015)."

8.P2, Line 16-18, Please cite the literature, doi: 10.5194/acp-15-12581-2015.

Response: We have read that paper and now cite it. Please see it in the answer for the above question.

9.P2, Line 24, 'the other is based on the field observations to apportion BC into different sources through a certain data analytical method.' Please add appropriate literature.

Response: We have re-written this text, and now it reads as follows:

> "Several studies have assessed the contributions of different BC sources through model simulations or isotopic methods. For example, Zhang et al. (2015) investigated BC sources for different parts of the TP by using a chemical transport model and a source tagging approach, and they found that the contributions of BC sources varied among regions and with the seasons. Li et al., (2016) used filter sampling and carbon isotopes ($\Delta^{14}C$ and $\delta^{13}C$) to determine the BC from fossil fuels and biomass burning in several areas of the TP."

10.P2, Line 25, 'transport to TP' should be changed to 'transport to the TP'.

Response: We have corrected and add the article "the" into TP in the revised version.

11.P3, Line 5, 'are advantageous to capturing' should be changed to 'are advantageous to capture'.

Response: We revised the sentence

"A major disadvantage of filter-based measurements is they are constrained by low time resolution, and this makes it challenging to capture the detailed evolution of pollution events."

12.P3, Line 10, 'cross-section (MAC) used in the model.' Please add appropriate literature.

Response: We have added the relevant literature:

"The accuracy of the 'aethalometer model' relies on the input parameters, including the Ångström exponents (AAE) and BC mass absorption cross-sections (MAC_{BC}) of different sources (Zotter et al., 2017)."

13. P4, Line 11, 'on the rooftop of' should be changed to 'at on the rooftop of'.

Response: We have corrected "on" into "at". The sentence now reads

"Intensive field measurements were made at the rooftop of a building (~10 m above the ground) at the Lijiang Astronomical Station, Chinese Academy of Sciences (3260 m above sea level, 100°1'48"E, 26°41'24"N), Gaomeigu County, Yunnan Province, China (Fig. 1) from 14 March to 13 May 2018."

14. P4, Line 15, 'the radiative effect' should be changed to 'the radiative effects'.

Response: We have changed all "radiative effect" into "radiative effects" in the revised version.

15. P5, Line 4, 'was resolved using' should be changed to 'was resolved by using'.

Response: We have changed the sentence as below:

"A dual-spot technique for the aethalometer measurements was used to compensate for non-linearity, while a factor of 2.14 was used to correct for the artifacts caused by the quartz filters (Drinovec et al., 2015)."

16. P8, Line 10, 'the number of the endpoints' should be changed to 'the number of endpoints'.

Response: We have deleted "the" before endpoints in the sentence:

"where m_{ij} is the number of endpoints associated with BC mass concentration higher than the set criterion;"

17. P9, Line 8, 'model is elaborated in Ricchiazzi and Yang, (1998)' should be changed to 'model was elaborated in Ricchiazzi and Yang (1998)'.

Response: We have corrected the tense as follows:

"The direct radiative effects (DRE) of source-specific BC were estimated with the widely used Santa Barbara DISORT Atmospheric Radiative Transfer (SBDART) model—a detailed description of which may be found in Ricchiazzi and Yang (1998)."

18. P10, Line 15, delete 'which is' before 'within a relative boarder range'. P10, Line 18, delete 'which was' before 'over two times'. In addition, it is necessary to pay attention to the tense errors, which often appear throughout the manuscript.

Response: Thanks for pointing out the error in tense. The paper has been edited and thoroughly revised, and the problems with tense should have been corrected. The sentences were changed to

"That was within the relatively broad range of $AAE_{biomass}$ (1.2–3.5) determined by other methods (e.g., $\triangle^{14}C$ and organic tracers) in previous studies (Sandradewi et al., 2008; Helin et al., 2018; Harrison et al., 2012; Zotter et al., 2017). The estimated average $MAC_{BC}(880)_{biomass}$ was 10.4 $m^2\ g^{-1}$; this is more than twice the value for uncoated BC particles suggested by Bond and Bergstrom (2006) ($MAC_{BC}(880)_{uncoated}$ = 4.7 $m^2\ g^{-1}$, extrapolated from 550nm to 880 nm by assuming AAE_{BC} = 1.0)."

19. P10, Line 19, Line 85, the comma before '(2006)' should be deleted.

Response: We corrected this mistake:

"The estimated average $MAC_{BC}(880)_{biomass}$ was 10.4 $m^2\ g^{-1}$; this is more than twice the value for uncoated BC particles suggested by Bond and Bergstrom (2006) ($MAC_{BC}(880)_{uncoated}$ = 4.7 $m^2\ g^{-1}$, extrapolated from 550nm to 880 nm by assuming AAE_{BC} = 1.0)."

20. P11, Line 5, 'may be relation with' should be changed to 'may be related with' or 'may have relation with'.

Response: We corrected this:

"Although unleaded gasoline has been used extensively in China since 2005, a considerable portion of the Pb in the environment is still associated with vehicle-related particles, especially from the wear of metal alloys (Hao et al., 2019)."

21. P12, Line 26, 'This suggests and' should be changed to 'This suggests that'.

Response: We have changed the sentence as following:

"One can infer from this that biomass-burning emissions were responsible for the high BC loading episode during the campaign."

22. P14, Line 12, 'the mainland China' should be changed to 'mainland China' or 'the mainland of China'.

Response: We have corrected this mistake in the revised manuscript:

"The air masses associated with Cluster 3 originated from the interior of China, and this group had the lowest BC mass concentrations of the three clusters, 0.4 ± 0.1 μg m^{-3}. This third cluster composed small fraction of total trajectories (2%), and none of them were identified as polluted, suggesting minor influences from mainland China during the campaign."

"The transportation sector has grown rapidly in mainland China (Liu, 2019a), and the regional transport of motor vehicle emissions may have been the cause for the observed diurnal variations in BC_{fossil} for Cluster 3."

Review of "Measurement report: Quantifying source contribution and radiative forcing of fossil fuel and biomass burning black carbon aerosol in the southeastern margin of Tibetan Plateau" (ACPD-2020-408, Liu et al)

Anonymous Referee #2

General comment: This paper reports on measurements and modeling regarding the contribution of fossil fuel and biomass burning sources to black carbon (BC) aerosols abundance and radiative forcing at a site south-east of the Tibetan Plateau. Methods used in the study are robust, and the results are sound. However, it is difficult to ascertain the novelty and actual contribution to the overall understanding of, for instance, how BC aerosols are affecting the Tibetan Plateau. In my opinion, authors may turn this study into a relevant one if they would consider using the data at hand by better explaining the reasons that make these data important for improved understanding. In its present form, detailed measurements and modeling are more suited for a technical report not suitable, in my opinion, for this prestigious journal.

Response: The authors appreciate the reviewer's valuable comments and suggestions, and we believe that the revised manuscript has been significantly improved after considering them. Below are point-to-point responses, and the modifications to the manuscript are marked.

Specific comments

(1) The text would improve in clarity and possibly be shorten if reviewed by a native English writer/speaker. Also, some results could be summarized in tables improving the readability of the text.

Response: We have had this manuscript polished by a native English speaking scientist. In addition, some results also are summarized in Table R1 (also see Table 1 in the revised manuscript) as suggested.

Table 1 Derived Ångström absorption exponents (AAE), Mass absorption coefficients (MAC) and percent source contribution of black carbon (BC) from difference sources

	AAE	MAC (m^2 g^{-1})	Mass concentration (μg m^{-3})	Contribution ratio
$BC_{biomass}$	1.7	10.4	0.4 ± 0.3	57%
$BC_{traffic}$	0.8	9.1	---	---
BC_{coal}	1.1	15.5	---	---
BC_{fossil}	0.9	12.3	0.3 ± 0.2	43%

(2) Abstract: Re-write according to suggestions below. What do we learn from this study? In what context is this useful? What is the novelty?

Response: As suggested, we have rewritten the abstract and clearly state the purpose, importance and novelty of the study. It now reads as follows:

"Anthropogenic emissions of black carbon (BC) aerosol are transported from Southeast Asia to the southwestern Tibetan Plateau (TP) during the pre-monsoon; however, the quantities of BC from different anthropogenic sources and the transport mechanisms are still not well constrained because there have been no high-time-resolution BC source apportionments. Intensive measurements were taken in a transport channel for pollutants from Southeast Asia to the southeastern TP during the pre-monsoon to investigate the influences of fossil fuels and biomass burning on BC. A receptor model coupled multi-wavelength absorption with aerosol species concentrations was used to retrieve site-specific Ångström exponents (AAE) and mass absorption cross-sections (MAC) for BC. An 'aethalometer model' that used those values showed that biomass burning had a larger contribution to BC mass than fossil fuels ($BC_{biomass}$ = 57% versus BC_{fossil} = 43%). The potential source contribution function indicated that $BC_{biomass}$ was transported to the site from northeastern India and northern Burma. The Weather Research and Forecasting model coupled with chemistry (WRF-Chem) model indicated that 40% of the $BC_{biomass}$ originated from Southeast Asia, while the highest BC_{fossil} was transported from the southwest of the sampling site. A radiative transfer model indicated that the average atmospheric direct radiative effects (DRE) of BC were +4.6 ± 2.4 W m^{-2} with +2.5 ± 1.8 W m^{-2} from $BC_{biomass}$ and +2.1 ± 0.9 W m^{-2} from BC_{fossil}. The DRE of $BC_{biomass}$ and BC_{fossil} produced heating rates of 0.07 ± 0.05 and 0.06 ± 0.02 K day^{-1}, respectively. This study provides insights into sources of BC over a transport channel to the southeastern TP and the influence of the cross-border transportation of biomass burning emissions from Southeast Asia during the pre-monsoon."

• *Introduction*

(3) Page 2, lines 13-14. In addition to characterizing source regions and their contributions to aerosol burden downwind it is also important to assess the timing in which this impact occur, how is the aging process, etc.

Response: We agree with the reviewer that timing and aging are also importation factors, so we have re-written this sentence in the revised manuscript. It now reads as follows:

> "Nonetheless, assessments of regional transport of bulk BC aerosol have not fully revealed the impacts of different BC emission sources because the optical properties and radiative effects of BC not only can vary among sources in complex ways but also can be affected by aging during transport (Tian et al., 2019; Zhang et al., 2019). Therefore, quantitative information on the contributions of different sources of BC over the TP is lacking, but it is critically needed for a better understanding the influence of anthropogenic emissions on its environment and climate."

(4) Page 2, lines 22-24. Uncertainties in modeling studies not only depend on uncertain emission estimates but also on how well chemistry, transport and deposition processes are represented, initial/boundary conditions, etc. It appears necessary to review other studies to get an idea of the uncertainty when using models to simulate long-range transport, particularly over complex terrain.

Response: We agree that the uncertainties of modeling method can be caused by the factors mentioned by reviewer and likely others. The complex terrain has impact on simulation of meteorological field over the Tibetan Plateau. We followed the reviewer's suggestion and have rewritten the relevant paragraph in the revised manuscript; it now reads as follows:

> "On the other hand, the accuracy of model simulations is dependent on many factors, including uncertainties associated with initial particle parameters, aging processes, the accuracy of emission inventory, meteorological fields over the complex terrain, and the modules for chemistry and planetary boundary layer (PBL) dynamics, etc. (Koch et al., 2009; Madala et al., 2014; Vignati et al., 2010)."

(5) Page 3, lines 1-24. This is a lengthy discussion about distinguishing between biomass and fossil fuel black carbon according to multiple observational and methodological studies. Rather than listing the pros and cons of the different methods, it would be good to have a clearer idea of which is the method fit for purpose to be discussed in the work. For that, it is key to establish a clear purpose, and how this will help improving

understanding of a given phenomenon.

Response: Following the reviewer's suggestion, we have rewritten the introduction in the revised manuscript and presented a clear explanation as to why we chose the online method, including why and how we optimized the methods. To clarify the purpose of this research, we re-organized the last two paragraphs of the introduction. They now read as follows:

> "To make up for the deficiencies of filter-based analysis, BC source apportionments based on high-time resolution online data has been conducted in many locations but for the TP are limited. An 'aethalometer model' based on multi-wavelength absorption data is one of efficient approaches for distinguishing between BC from fossil fuel and biomass burning sources (Sandradewi et. al., 2008). Although it has been widely used elsewhere, this approach has not been applied to the TP. The accuracy of the 'aethalometer model' relies on the input parameters, including the Ångström exponents (AAE) and BC mass absorption cross-sections (MAC_{BC}) of different sources (Zotter et al., 2017). Limited information on site specific AAEs and MAC_{BC}s, lead most studies to rely on values taken from measurements made in other locations (e.g., Healy et al., 2017; Zhu et al., 2017). This results in unquantified uncertainties because the AAEs and MAC_{BC}s vary with specific fuel subtypes and combustion conditions (Wang et al., 2018; Tian et al., 2019). Therefore, site-dependent AAE and MAC_{BC} are essential for improving the reliability of BC source apportionment by the 'aethalometer model'.
>
> In this study, field measurements of BC were taken on the southeastern margin of the TP during the pre-monsoon. This region connects the high altitude TP with the low altitude Yungui Plateau and forms a transport channel for pollutants from Southeast Asia (Wang et al., 2019a), and it is an ideal region for investigating the impact of pollutant transport to the southeastern TP. A receptor model that combined multi-wavelength absorption with aerosol species concentrations was used to retrieve site-dependent AAEs and MAC_{BC}s. This was done to improve the 'aethalometer model' with the goal of obtaining a more accurate BC source apportionment. The primary objectives of this study were to (1) quantify the mass concentrations of BC from fossil fuel and biomass burning sources; (2) determine the impact of regional transport on source-specific BC; and (3) assess the radiative effects caused by BC from different sources. This study provides insights into the BC sources on southeastern TP and an assessment of their radiative effects during the pre-monsoon."

(6) Page 4, lines 1-6. You state that previous studies have dealt with radiative impacts of bulk BC, no distinguishing BC sources. Furthermore, you state that this study would

be unique as it provides the first estimate of BC radiative forcing split by source regions. However, you estimate the instantaneous forcing over one site which is, by definition, locally representative, and not necessarily climatically important. Other studies may have estimated bulk BC forcing but over much longer periods of time, and over large areas, including the Himalayan cryosphere. Hence, I urge the authors to make their study unique by better establishing the purpose of it.

Response: We appreciate this comment. Taking into consideration Comments 1–5, we have re-written the introduction to explain the purpose of our study and we deleted this paragraph in the revised manuscript. BC is an important atmospheric light-absorbing material that can have significant radiative effects. The SBDART model has been widely used to estimate the instantaneous radiative effects of BC based on the ground observations (Gharibzadeh et al., 2017; Rajesh et al., 2018; Panicker et al., 2010). Although data from only one site on the southeastern TP were collected (because of practical limitations in personnel, equipment, logistics, etc.), we believe that the unique geographic location of sampling site (i.e., transport channel) on TP make our results of considerable interest. In addition, due to paucity of studies that have separately quantified BC mass from biomass burning and fossil fuels on TP, we think that it is important to understand their radiative effects and potential influences on climate.

References:

Gharibzadeh M , Alam K , Abedini Y , et al. Monthly and seasonal variations of aerosol optical properties and direct radiative forcing over Zanjan, Iran, J. Atoms. Sol-Terr. Phy.,164,268-275, dx.doi.org/10.1016/j.jastp.2017.09.006, 2017

Panicker, A. S., Pandithurai, G., Safai, P. D., Dipu, S., and Lee, D.-I.: On the contribution of black carbon to the composite aerosol radiative forcing over an urban environment, Atmos. Environ., 44, 3066-3070, 10.1016/j.atmosenv.2010.04.047, 2010.

Rajesh, T. A., and Ramachandran, S.: Black carbon aerosols over urban and high altitude remote regions: Characteristics and radiative implications, Atmos. Environ., 194, 110-122, 10.1016/j.atmosenv.2018.09.023, 2018.

• *Methodology*

(7) Page 4, line 17. Improve the precision of attitude and longitude to allow a proper location of the site.

Response: Following the reviewer's suggestion, we have specified the attitude and longitude of the sampling site in the revised manuscript. It now reads as follows:

"Intensive field measurements were made at the rooftop of a building (~10 m above the ground) at the Lijiang Astronomical Station, Chinese Academy of Sciences (3260 m above sea level, 100°1'48"E, 26°41'24"N), Gaomeigu County, Yunnan Province, China (Fig. 1) from 14 March to 13 May 2018."

(8) Page 4, lines 18-19. As per your reference, Wang et al (2019a), your observation site is located along a "transportation channel". Describe the overall transport patterns affect. Is the period of observations representative of which transport/circulation pattern? An overall meteorological description is missing.

Response: In the pre-monsoon season when the southeastern margin of the TP is influenced by the westerly winds (Chan et al 2017; Niu et al., 2017), a pathway for the cross border transport of emissions from southeast Asia to the TP. The sampling period for this study was from March to May and therefore in the pre-monsoon. In the revised manuscript, we have added some information about the 'transport channel'. It now reads as follows:

"During the campaign, westerly winds created a potential pathway for cross border transport from southeast Asia to southwest China. During the study, the average relative humidity and temperature were 80% ± 20% and 7.6 ± 3.2℃, respectively; the mean wind speed near surface was 5.4 ± 2.1 m s^{-1}, and the winds were mainly from the west and southwest."

References:

Chan, C. Y., Wong, K. H., Li, Y. S., Chan, Y., and Zhang, X. D.: The effects of Southeast Asia fire activities on tropospheric ozone, trace gases and aerosols at a remote site over the Tibetan Plateau of Southwest China, Tellus B , 58B, 310-318, 10.1111/j.1600-0889.2006.00187.x, 2017

Niu H., Kang., S., Zhang, Y., Shi, X., Shi., X., Wang S., Li, G., Yan, X., Pu, T. He, Y., Distribution of light-absorbing impurities in snow of glacier on Mt. Yulong, southeastern Tibetan Plateau, Atmos. Res., 197, 474-484, 10.1016/j.atmosres.2017.07.004, 2017.

(9) Page 4, lines 19-20. You say that the population surrounding your observational site is small. Small compared to what? Then you go onto establishing that limited anthropogenic activities are found there. However, your results show a non-negligible contribution. The site should be better described, including a brief description of aerosol sources.

Response: At the sampling site, the influence of anthropogenic activities is limited due to the low population density and lack of industries. The local emissions have small effects on the BC source apportionment results compared with the contributions of fossil fuel BC from two highways (5.5 km from the sampling site) and transport from the border with Burma. Following the reviewer's suggestion, we have added some information about the possible anthropogenic emissions in the surrounding area of the sampling site. The revised manuscript now reads as follows:

> "The sampling site is 3–5 km from Gaomeigu village, which has 27 households and 110 residents. Villagers there rely on farming for their livelihoods, and biomass is the primarily residential fuel (Li et al, 2016). There are no large industries near the village and traffic is light. However, two highways (Hangzhou-Ruili Expressway and Dali-Nujiang Expressway) are located ~5.5 km to the west of the sampling site."

(10) Page 7, section 2.5. HYSPLIT can be used with large-scale (synoptic) meteorological fields. Do you have an assessment of how well this approach works over complex terrain?

Response: The meteorological data used in this study were obtained from the Global Data Assimilation System (GDAS) and had a spatial resolution of 1°×1°. The HYSPLIT model converted the vertical layers from the original coordinate system into its own terrain-following coordinate system (sigma) and directly used the data contained in meteorological files for the trajectory calculations (Draxler and Hess, 1997). The surface in the terrain-following coordinate system is consistent with the ground, and that solves the problem of modelling near mountainous areas (Phillips, 1965). Furthermore, this method has been used over complex terrain with various meteorological data in a number of studies (Burley and Bytnerowicz 2011; Wang et al., 2015; Wang et al.,2019; Qu et al 2015 and Khan et al., 2010).

To determine if the trajectory would be impacted by the surface rising, we also ran calculations at heights of 150m and 1000m in addition to 500m (Figure R1). The results showed that directions were similar, particularly between the results at150m and at 500m. We finally decided to use the 500m results because greater heights be higher than the height at which the samples were collected, and 500m is generally representative of the average planetary boundary height at the site (~600m).

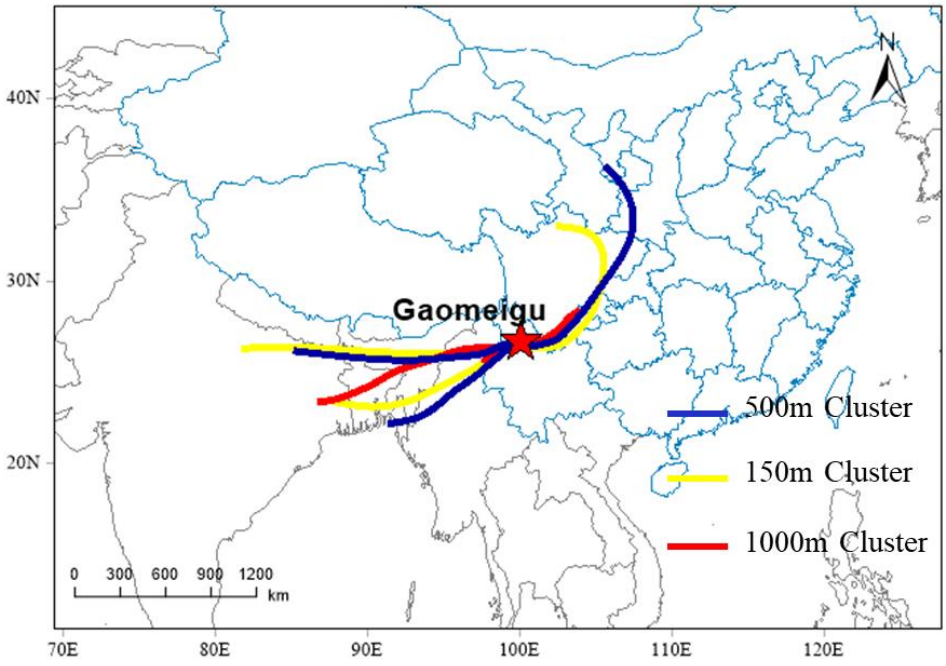

Figure R1. the blue lines represent the clusters at 500m height, the yellow lines represent the clusters at 150m height, the red lines represent the cluster at 1000m height.

References:

Burley J D , Bytnerowicz A . Surface ozone in the White Mountains of California, Atmospheric Environment, 45, 4591-4602, 10.1016/j.atmosenv.2011.05.062, 2011.

Chengkai Qu, Xinli Xing, Stefano Albanese, et al. Spatial and seasonal variations of atmospheric organochlorine pesticides along the plain-mountain transect in central China: Regional source vs. long-range transport and air – soil exchange, Atmos. Environ. 122, 31-40, 10.1016/j.atmosenv.2015.09.008, 2015.

Draxler, R., and Hess, G.: An overview of the HYSPLIT_4 modelling system for trajectories, Aust. Meteorol. Mag., 47, 1998.

Khan A J , Li J , Dutkiewicz V A , et al. Elemental carbon and sulfate aerosols over a rural mountain site in the northeastern United States: Regional emissions and implications for climate change, Atmos. Environ., 44, 2364-2371, 10.1016/j.atmosenv.2010.03.025, 2010.

Phillips N.A. a coordinate system having some special advantages for numerical forecasting, Shorter contributions, J. Atmos. Sci., 14, 184-185, 1957.

Wang, Q. Y., Huang, R. J., Cao, J. J., Tie, X. X., Ni, H. Y., Zhou, Y. Q., Han, Y. M., Hu, T. F., Zhu, C. S., Feng, T., Li, N., and Li, J. D.: Black carbon aerosol in winter northeastern Qinghai–Tibetan Plateau, China: the source, mixing state and optical property, Atmos. Chem. Phys., 15, 13059-13069, 10.5194/acp-15-13059-2015, 2015.

Wang, Q., Han, Y., Ye, J., Liu, S., Pongpiachan, S., Zhang, N., Han, Y., Tian, J., Wu, C., Long, X., Zhang, Q., Zhang, W., Zhao, Z., and Cao, J.: High Contribution of Secondary Brown Carbon to Aerosol Light Absorption in the Southeastern Margin of Tibetan Plateau, Geophys. Res. Lett., 46, 4962-4970, 10.1029/2019gl082731, 2019.

(11) Why do you choose 3-day back trajectories instead of 2 or 5 days?

Response: Studies have indicated that BC lifetime varies from 3.3 to 12 days in the atmosphere (Liu et al., 2011 and references therein). The BC lifetime depends on many factors such as morphology, size, mixing state, aging condition, and meteorological conditions. It is not possible to know the exact lifetime of the BC sampled at the study site, and therefore, we chose the lowest value for the BC lifetimes to minimize the effects of BC deposition during transport to the site. In addition, the 3-day backward trajectories also have been widely used in previous studies to investigate BC transport pathways (e.g., Wang et al., 2018; Verma et al., 2010).

References:

Liu, J., Fan, S., Horowitz, W. L., Levy, H., 116, Evaluation of factors controlling long - range transport of black carbon to the Arctic, J. Geophys. Res., doi:10.1029/2010JD015145, 2011.

Verma, R. L., Sahu L. K., Kondo, Y., Takegawa, N., Han, S., Jung, J. S., Kim, Y., J., Fan, S., Sugimoto, N., Shammaa, M. H., Zhang, Y., H., and Zhao, Y.: Temporal variations

of black carbon in Guangzhou, China, in summer 2006, Atmos. Chem. Phys., 10, 6471–6485, 10.5194/acp-10-6471-2010, 2010.

Wang, Q., Cao, J., Han, Y., Tian, J., Zhu, C., Zhang, Y., Zhang, N., Shen, Z., Ni, H., Zhao, S., and Wu, J.: Sources and physicochemical characteristics of black carbon aerosol from the southeastern Tibetan Plateau: internal mixing enhances light absorption, Atmos. Chem. Phys., 18, 4639-4656, 10.5194/acp-18-4639-2018, 2018.

• *Results and discussion*

(12) Page 11, lines 20-25. Your BC aerosol appears to have aged. Can't you use your WRF-Chem simulations to attempt providing further insights on this issue?

Response: We thank the reviewer providing us with this suggestion. However, BC is usually considered as chemically inert in the atmosphere (Bond et al., 2013), and the WRF-Chem model only accounts for physical processes of BC in the atmosphere, such as the wet and dry deposition. Although we concluded that BC underwent substantial aging, the objective of the study was to apportion the BC sources, and that did not include contributions from materials coating the BC. Moreover, due to the limitation of the measurement methods in this study, we could not obtain quantitative information regarding BC aging, which would have been the best way to constrain the model simulation. Therefore, the aging of BC is something that would be better addressed in future studies.

References:

Bond, T. C., Doherty, S. J., Fahey, D. W., Forster, P. M., Berntsen, T., DeAngelo, B. J., Flanner, M. G., Ghan, S., Kärcher, B., Koch, D., Kinne, S., Kondo, Y., Quinn, P. K., Sarofim, M. C., Schultz, M. G., Schulz, M., Venkataraman, C., Zhang, H., Zhang, S., Bellouin, N., Guttikunda, S. K., Hopke, P. K., Jacobson, M. Z., Kaiser, J. W., Klimont, Z., Lohmann, U., Schwarz, J. P., Shindell, D., Storelvmo, T., Warren, S. G., and Zender, C. S.: Bounding the role of black carbon in the climate system: A scientific assessment, J. Geophys. Res.-Atmos., 118, 5380-5552, 10.1002/jgrd.50171, 2013.

○ *Page 12, section 3.2.*

(13) Some of your results could be better appreciated if summarized in a table.

Response： As suggested, results have been summarized in to a table. Please see the response of comment 1 above.

(14) You make multiple references to FigS3. Maybe it is better to bring it to the main manuscript. If so, it could be useful to split the graphs for daytime and nighttime periods as it would better fit with Figure 2.

Response: The mass concentrations of levoglucosan and benzothiazolone were obtained from 24 h filter samples, and so we cannot compare daytime versus nighttime periods. Note that the online BC data were integrated to match each filter sampling times. We did follow the reviewer's suggestion and combined Fig. S3 with Fig. 2 in the revised manuscript (also see Fig. R2 below).

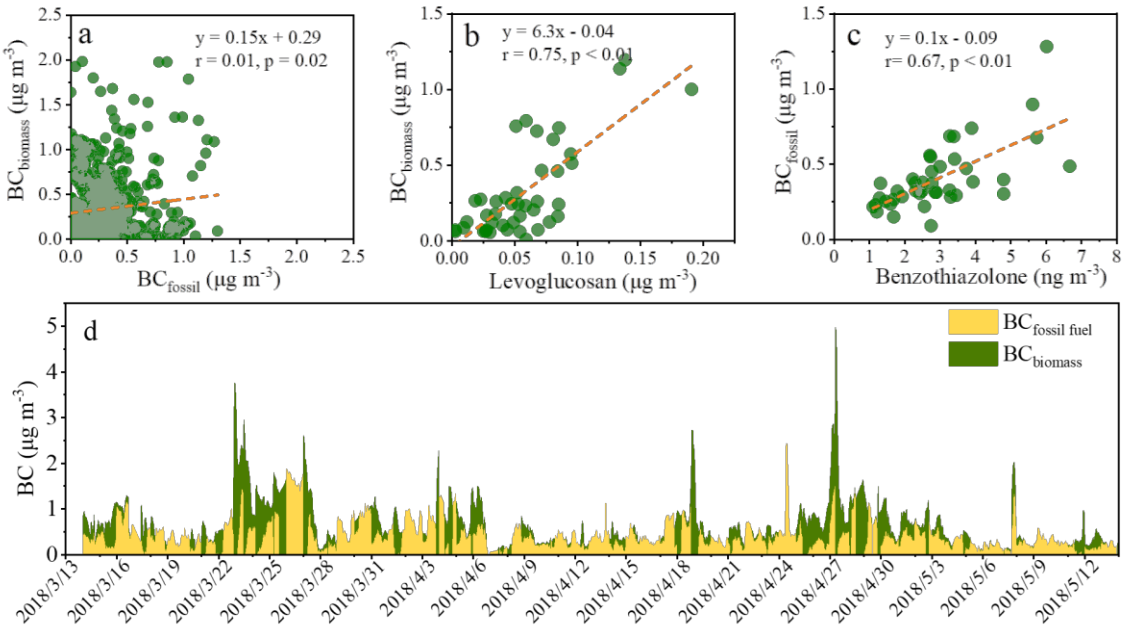

Figure R2. Scatter plots of (a) biomass burning BC ($BC_{biomass}$) versus fossil fuel combustion BC (BC_{fossil}), (b) $BC_{biomass}$ versus levoglucosan, and (c) BC_{fossil} versus benzothiazolone. $BC_{biomass}$ and BC_{fossil} represent black carbon aerosol contributed by biomass burning and fossil fuel sources, respectively. (d)Time series of hourly averaged mass concentrations of black carbon (BC) aerosol from biomass bunirng ($BC_{biomass}$) and fossil fuel sources (BC_{fossil}).

• *Conclusion*

(15) Stress the novelty, and make it explicit that the period studied correspond to a given set of transport/circulation patterns.

Response: We followed the reviewer's suggestion and rewrote the conclusions in the revised manuscript. It now reads as follows:

"This study quantified the source contributions of BC aerosol from fossil fuel and biomass burning at a site on the southeastern margin of the TP that represents a regional transport channel for air pollution during pre-monsoon. The study was conducted in pre-monsoon when the southeastern TP was heavily influenced by the air mass from southeast Asia. To reduce the uncertainties caused by interferences in absorption measurements (i.e. secondary absorption and dust) and assumptions relative to AAE and MAC_{BC}, the traditional 'aethalometer model' was optimized in two aspects. First, a BC-tracer method coupled with a minimum R-squared approach was applied to separate secondary absorption from the total absorption, and as a result, the interferences of absorption from secondary aerosols have been eliminated. Then, an optical source apportionment model that used primary multi-wavelength absorption and chemical species as inputs was used to derive site-dependent AAE and MAC_{BC} values—these minimize the uncertainties associated with prior assumptions on these parameters. The AAE (MAC_{BC}) calculated in this way was 0.9 (12.3 $m^2 g^{-1}$) for the fossil fuel source and 1.7 (10.4 $m^2 g^{-1}$) for biomass burning. The results of 'aethalometer model' that used these values showed that the average mass concentration of BC was 0.7 ± 0.5 μg m^{-3} of which 57% was from biomass burning and 43% from fossil fuels. Trajectory analysis showed that the $BC_{biomass}$ over the site was mainly driven by regional transport from northeastern India and Burma, while BC_{fossil} was primarily influenced by traffic emissions from areas surrounding the sampling site. Moreover, the WRF-Chem model indicated that biomass burning in Southeast Asia contributed 40% of the BC loadings over the southeastern margin of the TP. The SBDART model showed that a DRE of +4.6 ± 2.4 W m^{-2} for the total $PM_{2.5}$ BC, of which +2.5 ± 1.8 W m^{-2} was from $BC_{biomass}$ and +2.1 ± 0.9 W m^{-2} from BC_{fossil}. The results of our study provide useful information concerning the sources of BC over an atmospheric transport channel to the southeastern TP, and they highlight the importance of the cross-border transport of biomass burning emissions from Southeast Asia on the region during the pre-monsoon."

Measurement report: Quantifying source contribution of fossil fuels and biomass burning black carbon aerosol in the southeastern margin of Tibetan Plateau

Huikun Liu[1,2,3], Qiyuan Wang[1,2,3,4*], Li Xing[5], Yong Zhang[2], Ting Zhang,[2], Weikang Ran[2], Junji Cao[1,2,3,4*]

[1]State Key Laboratory of Loess and Quaternary Geology, Institute of Earth Environment, Chinese Academy of Sciences, Xi'an, 710061, China
[2]Key Laboratory of Aerosol Chemistry and Physics, Institute of Earth Environment, Chinese Academy of Sciences, Xi'an, 710061, China
[3]University of Chinese Academy of Sciences, Beijing, 100049, China
[4]CAS Center for Excellence in Quaternary Science and Global Change, Xi'an, 710061, China
[5]School of Geography and Tourism, Shaanxi Normal University, Xi'an, 710119, China

Correspondence to: Qiyuan Wang (wangqy@ieecas.cn) and Junji Cao (cao@loess.llqg.ac.cn)

Abstract.

Anthropogenic emissions of Black carbon (BC) aerosol are transported from Southeast Asia to the southwestern Tibetan Plateau (TP) during the pre-monsoon; however, the quantities of BC from different anthropogenic sources and the transport mechanisms are still not well constrained because there have been no high-time-resolution BC source apportionments. Intensive measurements were taken in a transport channel for pollutants from Southeast Asia to the southeastern margin of TP during the pre-monsoon to investigate the influences of fossil fuels and biomass burning on BC. A receptor model coupled multi-wavelength absorption with aerosol species concentrations was used to retrieve site-specific Ångström exponents (AAE) and mass absorption cross-sections (MAC) for BC. An 'aethalometer model' that used those values showed that biomass burning had a larger contribution to BC mass than fossil fuels ($BC_{biomass}$ = 57% versus BC_{fossil} = 43%). The potential source contribution function indicated that $BC_{biomass}$ was transported to the site from northeastern India and northern Burma. The Weather Research and Forecasting model coupled with chemistry (WRF-Chem) model indicated that 40% of $BC_{biomass}$ originated from Southeast Asia, while the high BC_{fossil} was transported from the southwest of sampling site. A radiative transfer model indicated that the average atmospheric direct radiative effects (DRE) of BC was +4.6 ± 2.4 W m^{-2} with +2.5 ± 1.8 W m^{-2} from $BC_{biomass}$ and +2.1 ± 0.9 W m^{-2} from

删除了: and radiative forcing

删除了: plays a vital role in disturbing the balance of ecosystem and climate stability of

删除了: An

删除了: i

删除了: campaign

删除了: was carried out from 14th March to 12th May 2018 in

删除了: sources of

删除了: and their radiative effects

删除了: To do so,

删除了: a

删除了: improved

删除了: was

删除了: t

删除了: o distinguish and apportion BC into fossil fuel combustion source and

删除了: source

删除了: To minimize the uncertainty associated with the 'aethalometer model', a receptor model coupling multi-wavelength absorption with chemical species was used to retrieve the site-dependent Ångström exponent (AAE) and BC mass absorption cross-section (MAC). The results show that the AAEs and BC MACs at wavelength of 880 nm were 0.9 and 12.3 m^2 g^{-1} for fossil fuel source and 1.7 and 10.4 m^2 g^{-1} for biomass burning, respectively. Based on these parameters, the fossil fuel source-related BC (BC_{fossil}) was estimated 43% of the total BC and the rest 57% was from biomass burning ($BC_{biomass}$) during the campaign.

删除了: results from a regional chemical dynamical model reveal

删除了: high

删除了: contributed

删除了: the

删除了: and the Southeast Asia can explain

删除了: .

删除了: T

删除了: mainly identified

删除了: e

删除了: a

删除了: estimated

删除了: forcing

删除了: on average, including

删除了: ,

BC_{fossil}. The DRE of $BC_{biomass}$ and BC_{fossil} produced heating rates of 0.07 ± 0.05 and 0.06 ± 0.02 K day^{-1}, respectively. This study provides insights into sources of BC over a transport channel to the southeastern TP and the influence of the cross-border transportation of biomass burning emissions from Southeast Asia during the pre-monsoon.

删除了: ,

删除了: which correspond to and

删除了: Our study will be useful for improving our understanding in BC sources on the TP and their climatic effect.

1 Introduction

The Tibetan Plateau (TP) is an important regulator of climate change in the northern hemisphere and it plays a crucial role in the functions of global ecosystem and climate stability (Liu et al., 2019b; Liu et al., 2020a). The TP is covered by one of the largest ice masses on Earth, and it has been called the water tower of Asia (Liu et al., 2020b). The glaciers on the TP are facing rapid retreat, however, and if unchecked, that could result in adverse effects on Asian hydrological cycle and Asian monsoon (Luo et al., 2020; Hua et al., 2019). In spring, the glaciers on the TP begin to melt as part of the natural hydrological cycle, but the increasing quantities of black carbon (BC) aerosol transported to the TP has accelerated this process (Bond et al., 2013) by causing a warming effect in atmosphere over the TP and enhancing the absorption of radiation on the surface of the glaciers (Ming et al., 2009).

The southern part of the TP is bounded by South Asia where air pollution often is severe (Chan et al. 2017). Several studies have shown that pollutants (including BC) from South Asia can be transported to the south of the TP along mountain-valleys, especially during the pre-monsoon (March–May) when southwestly winds prevail (e.g., Cao et al., 2010; Xia et al., 2011 Zhu et al., 2017; Niu et al. 2017). For example, Xia et al., (2011) analyzed satellite data and air mass trajectories and found that the TP, particularly the southern TP, was affected by pollutants carried by southwesterly winds from nearby regions in South Asia. In addition, numerous studies have shown that the high bulk BC mass loadings and the associated regional influences on the TP are related to transport from South Asia (Liu et al., 2015; Han et al., 2020; Cong et al., 2015; Wang et al., 2015). Nonetheless, assessments of regional transport of bulk BC aerosol have not fully revealed the impacts of different BC emission sources because the optical properties and radiative effects of BC not only can vary among sources in complex ways but also can be affected by aging during transport (Tian et al., 2019; Zhang et al., 2019). Therefore, quantitative

删除了: considered as a

删除了: (Yang et al., 2014)

删除了: It

删除了: s

删除了: system

删除了: which is known

删除了: (Immerzeel et al., 2010)

删除了: recently shows are rapidly retreating, which

删除了: lead to

删除了: (Wu et al., 2015)

删除了: Although the causes of glacier melting are complex,

删除了: loading on

删除了: an inescapable role in

删除了: (Yang et al., 2015). The BC deposited on glaciers increases ice melting

删除了: the enhanced radiation absorption on the surface

删除了: , which further influences the mass balance of glaciers

information on the contributions of different sources of BC over the TP is lacking, but it is critically needed for a better understanding the influence of anthropogenic emissions on its environment and climate.

Several studies have assessed the contributions of different BC sources through model simulations or isotopic methods. For example, Zhang et al. (2015) investigated BC sources for different parts of the TP by using a chemical transport model and a source tagging approach, and they found that the contributions of BC sources varied among regions and with the seasons. Li et al., (2016) used filter sampling and carbon isotopes ($\Delta^{14}C$ and $\delta^{13}C$) to determine the BC from fossil fuels and biomass burning in several areas of the TP. A major disadvantage of filter-based measurements is they are constrained by low time resolution, and this makes it challenging to capture the detailed evolution of pollution events. On the other hand, the accuracy of model simulations is dependent on many factors, including uncertainties associated with initial particle parameters, aging processes, the accuracy of emission inventory, meteorological fields over the complex terrain, and the modules for chemistry and planetary boundary layer (PBL) dynamics, etc. (Koch et al., 2009; Madala et al., 2014; Vignati et al., 2010). Nonetheless, these studies have been helpful for understanding the sources of BC over the TP.

To make up for the deficiencies of filter-based analysis, BC source apportionments based on high-time resolution online data has been conducted in many locations (e.g., Herich et al., 2011; Zhu et al., 2017; Rajesh and Ramachandran, 2018) but for the TP are limited. An 'aethalometer model' based on multi-wavelength absorption data is one of efficient approaches for distinguishing between BC from fossil fuel and biomass burning sources (Sandradewi et. al., 2008). The accuracy of the 'aethalometer model' relies on the input parameters, including absorption Ångström exponent (AAE) and BC mass absorption cross-section (MAC) of different sources (Zotter et al., 2017). Limited information on site specific AAEs and MAC_{BC}s lead most studies to rely on values taken from measurements made in other locations (e.g., Healy et al., 2017; Zhu et al., 2017). This results in unquantified uncertainties because the AAE and MAC_{BC} can vary with specific fuel subtypes and combustion conditions (Wang et al., 2018; Tian et al., 2019). Therefore site-dependent AAE and MAC_{BC} are essential for improving the reliability of BC source apportionment by the 'aethalometer model'.

删除了: The main paths for BC in glaciers are scavenged from atmosphere through dry and wet deposition (Ménégoz et al., 2014). Thus, exploring the source features of atmospheric BC on the TP is critical for further understanding its environmental and climatic effects. …As well known, BC is a byproduct from incomplete As well known, BC is a byproduct from incomplete combustion process of carbon contained fuels (e.g., fossil fuel and biomass) (Bond et al., 2013). Currently, the majority of the atmospheric BC studies on the TP focuses on characterizing the spatial and temporal distributions of bulk BC aerosol, and its regional sources (e.g., Rai et al., 2019; Wang et al., 2015). However, few studies shed light on the quantification of BC from different sources and their regional impacts. Owing to the various physicochemical characteristics, the climatic effects of BC produced by different sources could be divergent. Thus, it is important to understand the sources of BC on the TP. Among those limited available studies, they mainly focus on two aspects. One is obtaining the contribution fractions of different regions to the source-specific BC on the TP using modeling methods (Zhang et al., 2015); the other is based on the field observations to apportion BC into different sources through a certain data analytical method. The former approach has advantage in understanding the influence of BC regional transport to TP, but the result strongly depends on the accuracy of the emission inventory of different BC sources. The latter one can be achieved by multiple methods, for example, the filter-based approaches of isotope analysis (e.g., $\Delta^{14}C/\delta^{13}C$, Li et al., 2016). The isotope approach has a good accuracy in BC source apportionment, but the sampling time is usually as long as 24h or even longer to ensure the enough sample on filter to meet the requirement of detection limits of analyzer. Thus, this method is limited by its low time resolution and fails to capture the accurate time of pollution events occurred on the TP.

删除了: As well known, BC is a byproduct from incomplete process of carbon contained fuels (e.g., fossil fuel and biomass) (Bond et al., 2013). Currently, the majority of the atmospheric BC studies on the TP focuses on characterizing the spatial and tempora …

删除了: Online methods, on the contrary, are advantageous to capturing pollution events because of its high time resolution feature. Among them, a multi-wavelength optical method called aethalome …

删除了: Although

删除了: can apportion BC with a high time resolution, its robustness depends

删除了: selection of

删除了: used in the model

删除了: In current studies, most of them cited source-specific AAEs from previous publications and assumed the same BC MACs regardless of its difference in sources (e.g., Healy et al., 2017;Zhu …

删除了: i

删除了: ntroduces great

删除了: ,

删除了: even for the same type of emission source,

设置了格式: 下标

删除了: To improve the accuracy, several studies tried to constrain the AAE values by a comparison between different source-generated BC and the source markers (e.g., levoglucosan) or by the ^{14}C meth …

设置了格式: 字体: (中文) Times New Roman, 英语(英国)

In this study, field measurements of BC were taken on the southeastern margin of the TP during the pre-monsoon. This region connects the high altitude TP with the low altitude Yungui Plateau and forms a transport channel for pollutants from Southeast Asia (Wang et al., 2019a), and it is an ideal region for investigating the impact of pollutant transport to the southeastern TP. a receptor model that combined with multi-wavelength absorption with aerosol species concentrations was used to retrieve site-dependent AAEs and BC MAC_{BC}s. This was done to improve the 'aethalometer model' with the goal of obtaining a more accurate BC source apportionment. The primary objectives of this study were to (1) quantify the mass concentrations of BC from fossil fuel and biomass burning sources; (2) determine the impact of regional transport on source-specific BC, and (3) assess the radiative effects caused by BC from different sources. This study provides insights into the BC sources on the southeastern TP and an assessment of their radiative effects during the pre-monsoon.

2 Methodology

2.1 Sampling site

Intensive field measurements were made at the rooftop of a building (~10 m above the ground) at the Lijiang Astronomical Station, Chinese Academy of Sciences (3260 m above sea level, 100°1'48"E, 26°41'24"N), Gaomeigu County, Yunnan Province, China (Fig. 1) from 14 March to 13 May 2018. During the campaign, westerly winds created a potential pathway for cross border transport from southeast Asia to southwest China. During the study, the average relative humidity and temperature were 80% ± 20% and 7.6 ± 3.2℃, respectively; the mean wind speed near surface was 5.4 ± 2.1 m s^{-1}, and the winds were mainly from the west and southwest. The sampling site is 3–5 km from Gaomeigu village, which has 27 households and 110 residents. Villagers there rely on farming for their livelihoods, and biomass is the primarily residential fuel (Li et al, 2016). There are no large industries near the village and traffic is light. However, two highways (Hangzhou-Ruili Expressway and Dali-Nujiang Expressway) are located ~5.5 km to the west of the sampling site.

删除了: BC is recognized as the second largest anthropogenic warming agent globally after carbon dioxide, and its radiative effect varies largely with different areas (Bond et al., 2013). Currently, regional modeling and observation-based methods have been used in assessing BC radiative forcing on the TP. In this regard, most studies concentrate on the areas of longitude between 72 – 86° (e.g., Rajesh and Ramachandran, 2018; Bhat et al., 2017; Dumka et al., 2013; Singh et al., 2018). These studies focus on the radiative effect caused by bulk BC aerosol and some of them indicate that BC can account for 55 – 70% of the composite aerosol atmospheric radiative forcing (Panicker et al., 2010; Srivastava et al., 2012; Sreekanth et al., 2007). As summarized above, owing to the lack of studies regarding BC source apportionment on the TP, to our knowledge, there is no literature referring to the impacts of source-specific BC on the radiative forcing at present.

删除了: coupling

删除了: and chemical species

删除了: utilized

删除了: the

设置了格式: 下标

删除了: ,

删除了: and then an improved aethalometer model was used to determine the mass portions

删除了: aerosol

删除了: combustion source

删除了:

删除了: on the TP

删除了: R

删除了: of

删除了: was further explored by models. Finally,

删除了: were evaluated using a radiative transfer model.

删除了: Our

删除了: impacts

删除了: on regional climate

删除了: observation from 14 March to 13 May 2018 were conducted on the rooftop of. a 10m height building above the ground (3260 m a. s.l.) in …

删除了: 100.03°E, 26.70°N

删除了: which was located in

删除了: S

2.2 Online and offline measurements

Aerosol light absorption coefficients at multiple wavelengths ($b_{abs}(\lambda)$, λ = 370, 470, 520, 590, 660, 880, and 950 nm) were retrieved with the use of a model AE33 aethalometer (Magee Scientific, Berkeley, CA, USA). The sampled particles were selected by a $PM_{2.5}$ cuff-off inlet (SCC 1.829, BGI Inc. USA) and dried with a Nafion® dryer (MD-700-24S-3; Perma Pure, Inc., Lakewood, NJ, USA) , and the flowrate of the sampler is 5 L min^{-1}. Detailed operating principles of the AE33 aethalometer can be found in Drinovec et al. (2015). Briefly, light at wavelengths (λ) = 370, 470, 520, 590, 660, 880, and 950 nm emitted from diodes is used to irradiate aerosol deposition spots on the filters. The light attenuation produced by the captured particles is measured with optical detectors. Non-linear loading and filter matrix scattering effects are common issues for filter-based absorption measurements (Coen et al., 2009). A dual-spot technique for the aethalometer measurements was used to compensate for non-linearity, while a factor of 2.14 was used to correct the artifacts caused by quartz filters (Drinovec et al., 2015).

A photoacoustic exinctiometer (PAX, Droplet Measurement Technology, Boulder, CO, USA) was used to determine the aerosol light scattering and absorption coefficient ($b_{scat}(532)$ and $b_{abs}(532)$, respectively) which were used to calculate the single scattering albedo (SSA = $b_{scat}/(b_{scat}+b_{abs})$) at λ = 532 nm. The b_{scat} was measured using a wide-angle (5 – 175°) integrating reciprocal nephelometer in the scattering chamber. The $b_{abs}(532)$, was measured simultaneously with an intracavity photoacoustic technique in the acoustic chamber. Detailed description of PAX may be found in Carrico et al. (2018). During the campaign, the selected concentrations of ammonium sulphate and freshly-generated propane soot were used to calibrated the $b_{scat}(532)$ and $b_{abs}(532)$ measurements, respectively. Details regarding the calibration procedure are in Wang et al. (2018).

Daily $PM_{2.5}$ filters were collected for the analysis of selected chemical species. Organic carbon (OC) and elemental carbon (EC) were determined using a thermal/optical carbon analyser (Atmoslytic Inc., Calabasas, CA, USA). water-soluble potassium ion (i.e., K^+), and levoglucosan were analysed with the use of an ion chromatograph (Dionex Inc., Sunnyvale, CA, USA).The inorganic elements (i.e., S. Ca, Ti, Mn, Fe, Cu, As, Br, Pb, Zn) were measured using an energy-dispersive X-ray fluorescence spectrometry(Epsilon 5 ED-XRF, PANalytical B.V., Netherlands). Finally, an organic marker of benzothiazolone was determined using a high-performance liquid chromatography (Series 1200; Agilent

删除了: **The location connects high altitude TP with low altitude Yungui Plateau forming a transportation channel for pollutants from Southeast Asia (Wang et al., 2019a). The population of Gaomeigu County is small, and limited anthropogenic activities were found around the sampling site.**

删除了: as…retrieved with the use of aby…model AE33 aethalometer (Magee Scientific, Berkeley, CA, USA) at multiple wavelengths covering from near-ultraviolet to near-infrared… The sampled particles were selected by a $PM_{2.5}$ cuff-off inlet (SCC 1.829, BGI Inc. USA) and dried with a Nafion® dryer (MD-700-24S-3; Perma Pure, Inc., Lakewood, NJ, USA) , and theusing…a …lowrate of the sampler is 5 L min^{-1}. Detailed operatingoperation…principles of the AE33 aethalometer can be foundhas been…elaborated …n Drinovec et al. (2015). Briefly, light at wavelengths (λ)λ…= 370, 470, 520, 590, 660, 880, and 950 nm emitted from diodes is used were utilized…to irradiate aerosol deposition spots on thethe…filters deposition spot…,…and …t…e produced …ight attenuation producedis detected…by the captured particles is measured with optical detectors. Non-linear loading and filter matrix scattering effects are common issues forof…filter-based absorption measurements (Coen et al., 2009). The former issue was resolved using …a…dual-spot compensation …echnique for the aethalometer measurements was used to compensate for non-linearity, embedded in AE33 aethalometer …hile a factor of 2.14 was used to correct the artifactslatter issue …

删除了: (b_{scat}) …nd $b_{abs}(532)$, respectively) b_{abs}…which were used to calculateas well as obtaining…the single scattering albedo (SSA = $b_{scat}/(b_{scat}+b_{abs})$) at λ = 532 nm wavelength of 532 nm… The b_{scat} was measured using a wide-angle (5 – 175° degree… integrating reciprocal nephelometer in the scattering chamber.;…The $b_{abs}(532)$ and the b_{abs}…was measured simultaneously with an intracavity photoacoustic technique in the acoustic chamber. More …d…tailed description of PAX maycan…be found in Carrico et al. (2018). During the campaign, the selected b_{scat} and b_{abs} measurements were calibrated by different …oncentrations of ammonium sulphate and freshly-generated propane soot were used to calibrated the $b_{scat}(532)$ and $b_{abs}(532)$ measurements, respectively. Details regarding the Detailed…calibration procedure are has been elaborated …

删除了: Twenty-four-hour…$PM_{2.5}$ filterssamples…were collected for the analysis of selected chemical species. Organic carbon (OC) and elemental carbon (EC) were determined using a thermal/optical carbon analyser (Atmoslytic Inc., Calabasas, CA, USA). from 10:00 local time to 10:00 the next day on quartz fibre filters (8 × 10 inches, QM/A™; Whatman, Middlesex, UK) by a high-volume sampler (Tisch Environmental, Inc., USA) with an operating flowrate of 1.05 m^3 min^{-1}. The blank filters before sampling and the loaded filters after sampling were weighted to obtain PM2.5 mass in a thermostatic room using a Sartorius MC5 electronic microbalance (Sartorius, Göttingen, Germany). The sampled filters were well-stored in a refrigerator at -4°C to reduce the loss of volatile substances prior to chemical analysis. The chemical species involved carbonaceous matter (i.e., organic carbon (OC) and elemental carbon (EC)), …ater-soluble potassiuminorganic…ions…(i.e., K^+), and levoglucosan were analysed with the use of an ion chromatograph (Dionex Inc., Sunnyvale, CA, USA).The inorganic elements (i.e., S. Ca, Ti, Mn, Fe, Cu, As, Br, Pb, Zn),…which …ere measured using andetermined by thermal/optical carbon analyser, ion chromatograph, and…energy-dispersive X-ray fluorescence spectrometry(Epsilon 5 ED-XRF, PANalytical B.V., Netherlands), respectively… Finally, an Furthermore, …rganic marker ofs of levoglucosan and …

Technology, Santa Clara, CA). Detailed descriptions of the chemical analyses are given in Text S1 in the Supplementary Material.

2.3 BC source apportionment

The 'aethalometer model' proposed by Sandradewi et. al, (2008) was optimized by excluding the $b_{abs}(370)$ contributed by the secondary aerosols and soil dust ($b_{abs}(370)_{secondary}$ and $b_{abs}(370)_{dust}$, respectively). The The formulae used for the 'aethalometer model' were as follows:
as follows:

$$\frac{b_{abs}(370)_{fossil}}{b_{abs}(880)_{fossil}} = \left(\frac{370}{880}\right)^{-AAE_{fossil}} \quad (1)$$

$$\frac{b_{abs}(370)_{biomass}}{b_{abs}(880)_{biomass}} = \left(\frac{370}{880}\right)^{-AAE_{biomass}} \quad (2)$$

$$b_{abs}(880) = b_{abs}(880)_{fossil} + b_{abs}(880)_{biomass} \quad (3)$$

$$b_{abs}(370) = b_{abs}(370)_{fossil} + b_{abs}(370)_{biomass} + b_{abs}(370)_{secondary} + b_{abs}(370)_{dust} \quad (4)$$

where AAE_{fossil} and $AAE_{biomass}$ are the AAEs for emissions of fossil fuel contribution and biomass burning. These were retrieved through an optical source apportionment and discussed in section 3.1. $b_{abs}(370)$ and $b_{abs}(880)$ are the measured b_{abs} at λ = 370 and 880 nm, respectively; The absorption coefficients for fossil fuel are $b_{abs}(370)_{fossil}$ and $b_{abs}(880)_{fossil}$ while those for biomass burning sources are $b_{abs}(370)_{biomass}$ and $b_{abs}(880)_{biomass}$. A source apportionment of the optical data was used to calculate $b_{abs}(370)_{dust}$ as discussed in section 3.1 while $b_{abs}(370)_{secondary}$ was estimated using a BC-tracer method combined with a minimum *R*-squared approach as described by Wang et al. (2019a).

After obtaining $b_{abs}(880)_{fossil}$ and $b_{abs}(880)_{biomass}$, the mass concentrations of BC from fossil fuel combustion and biomass burning (BC_{fossil} and $BC_{biomass}$, respectively) were estimated as follows:

$$BC_{fossil} = \frac{b_{abs}(880)_{fossil}}{MAC_{BC}(880)_{fossil}} \quad (5)$$

$$BC_{biomass} = \frac{b_{abs}(880)_{biomass}}{MAC_{BC}(880)_{biomass}} \quad (6)$$

删除了: were measured using an ion chromatograph and a high-performance liquid chromatography (HPLC), respectively
删除了: More
删除了: d
删除了: information regarding above measurements is shown
删除了: supporting information
删除了: (
删除了: ,
删除了: improved
删除了: considering
删除了: caused
删除了: formation
删除了: Therefore,
删除了: t
删除了: b_{abs} of the BC generated from fossil fuel combustion and biomass burning were calculated
删除了: corresponding to
删除了: emissions
带格式的: 定义网格后不调整右缩进, 不调整西文与中文之间的空格, 不调整中文和数字之间的空格
删除了: which
删除了: derived
删除了: from
删除了: method as
删除了: are b_{abs} of fossil fuel BC at λ = 370 and 880 nm, respectively; ...
删除了: are b_{abs} of biomass-burning BC at λ = 370 and 880 nm, respectively; $b_{abs}(370)_{secondary}$ represents b_{abs} caused by secondary processes at λ = 370;
删除了: represents b_{abs} associated with soil dust at λ = 370, which was calculated in section 3.1. In this study, a
删除了: coupled
删除了: was used to retrieve the $b_{abs}(370)_{secondary}$ (Wang et al., 2019a):
$b_{abs}(370)_{secondary} = b_{abs}(370) - \left(\frac{b_{abs}(370)}{BC}\right)_{pri} \times$ [BC] (5)
where $\left(\frac{b_{abs}(370)}{BC}\right)_{pri}$ represents the $b_{abs}(370)$ associated with BC in the primary emissions(in unit of $m^2\ g^{-1}$), and [BC] denotes the mass concentration of BC in the atmosphere (in unit of $\mu g\ m^{-3}$), which was calculated with $b_{abs}(880)$ and EC loading. Detailed description of the $b_{abs}(370)_{secondary}$ calculation can be found in
删除了: calculating
删除了: based on Eqs. (1) – (5),
删除了: 6
删除了: 7

where $MAC_{BC}(880)_{fossil}$ and $MAC_{BC}(880)_{biomass}$ are the MAC_{BC}s at λ = 880 nm generated from fossil fuel combustion and biomass burning, respectively. The $MAC_{BC}(880)$s for the two sources were retrieved from a source apportionment of the optical data discussed in section 3.1.

2.4 Optical source apportionment

Optical source apportionments were obtained using a positive matrix factorization (PMF) model. The fundamental objective of PMF for applications such as ours is to resolve the chemical mass balance by separating data matrix into factor contributions and factor profiles as follows:

$$X_{ij} = \sum_{k=1}^{p} g_{ik} f_{kj} + e_{ij} \quad (7)$$

where X_{ij} represents the input matrix elements; p is the number of sources; g_{ik} is the source contribution of the kth factor to the ith sample; f_{kj} is the factor profile of jth species in the kth factor; and e_{ij} is representative of the residual. g_{ik} and f_{kj} are non-negative. The two matrices are resolved by minimizing the sum of squares of the normalized residuals as follows:

$$Q = \sum_{i=1}^{n} \sum_{j=0}^{n} \left[\frac{e_{ij}}{u_{ij}}\right]^2 \quad (8)$$

where Q represents the object function; and u_{ij} denotes the uncertainties of X_{ij}. The PMF version 5.0 (PMF5.0, from USEPA) was used for the analyses, and the optical parameters (primary b_{abs} at different wavelengths) and chemical species concentrations (including carbonaceous aerosols, inorganic elements, K^+, levoglucosan and organic markers) were used as model inputs for the optical source apportionment.

2.5 Trajectory-related analysis

To determine the influences of regional transport on BC at Gaomeigu, trajectory clusters were produced from hourly three-day backward-in-time air mass trajectories at 500 m above the ground level. The trajectories were calculated with the Hybrid Single-Particle Lagrangian Integrated Trajectory model (Draxler and Hess, 1998). The meteorological data were from Global Data Assimilation System (GDAS, https://www.ready.noaa.gov/gdas1.php), which take into account the influences of terrain. As we focused on differentiating and clustering the main spatial features of the incoming trajectories, an angle-oriented

删除了: MAC of BC
删除了: ,
删除了: which were retrieved
删除了: optical
删除了: as
删除了: The
删除了: o
删除了: was
删除了: realized via
删除了: principle
删除了: 8
删除了: 9
删除了: utilized
删除了: matter
删除了: both
删除了: to perform
删除了: regional transport to
删除了: analysis was
删除了: based on the
删除了: using
删除了: Since
删除了: directions of coming

distance definition was adopted in the cluster analysis. Details regarding the trajectory clustering methods can be found in Wang et al. (2018). For the investigations of the effects of transport on the chemical and optical properties of the BC aerosol, trajectories with BC mass concentration greater than 75th percentile were considered as polluted.

The potential source contribution function (PSCF) was used to identify the likely pollution regions that influenced BC loadings at Gaomeigu based on the back trajectories. The geographic region covered by the trajectories was overlaid by a of 0.5 × 0.5°(i, j) grid. The PSCF value of each grid was calculated as follows:

$$PSCF_{ij} = \frac{m_{ij}}{n_{ij}} \quad (9)$$

where m_{ij} is the number of endpoints associated with BC mass concentration higher than the set criterion; and n_{ij} is the total endpoints of the ijth cell. To improve the resolution of PSCF source identifications, the 75th percentile of each source's BC mass concentration was set as the criterion for a polluted sample (i.e., 0.6 μg m^{-3} for $BC_{biomass}$ and 0.45 μg m^{-3} for BC_{fossil}) (Cheng and Lin, 2001). Furtherrmore, arbitrary weighting factors (w_{ij}) were applied to different n_{ij} ranges to reduce the uncertainty caused by the small n_{ij} (Polissar et al., 1999), and they were defined by following the approach of Polissar et al. (2001):

$$W_{ij} = \begin{cases} 1 & 80 < N_{ij} \\ 0.7 & 20 < N_{ij} \le 80 \\ 0.42 & 10 < N_{ij} \le 20 \\ 0.05 & N_{ij} \le 10 \end{cases} \quad (10)$$

2.6 Regional chemical dynamical model

The Weather Research and Forecasting model coupled with chemistry (WRF-Chem) model was used to quantify the contribution of biomass-burning from Southeast Asian to BC mass at Gaomeigu. Detailed descriptions of the model configurations have been described in our previous publication (Xing et al., 2020). Briefly, the model resolution was 3 km × 3 km, and there were 320 grid cells. The domain included the southwest of China, southern and southeastern Asia, with a central at 100.03°E, 26.70°N. Thirty-five vertical layers has been set in the model from the ground surface to 50hPa. The BC emission inventory

删除了: The
删除了: d
删除了: ed
删除了: d
删除了: escription of the cluster analysis
删除了: To distinguish the pollution direction
删除了: the
删除了: y
删除了: over
删除了: was referred
删除了: a
删除了: trajectory
删除了: , otherwise was a clean one.
删除了: further
删除了: ward
删除了: apped
删除了: layer
删除了: 10
删除了: the
删除了: (Cheng and Lin, 2001)
删除了: pollution
删除了: criterion
删除了: an
删除了: as
删除了: it was
删除了: as follows (Polissar et al., 2001)
删除了: 1
删除了: contribution of
删除了: More
删除了: d
删除了: are
删除了: s in each of the latitude and longitude
删除了: was
删除了: concentrated in
删除了: South Asia, and Southeast
删除了: the
删除了: location
删除了: A

used for the model was based on the Asian anthropogenic emission inventory (that is MIX) for the year of 2010 (Li et al., 2017). The inventory has a spatial resolution of 0.25° × 0.25° and it included industry, power, transportation, and residential sources (e.g., fossil fuel and biofuel). The FINN fire inventory (Wiedinmyer et al., 2011) was used for the biomass-burning emission during the simulation.

2.7 Estimations of direct radiative effects and heating rate

The direct radiative effects (DRE) of source-specific BC were estimated with the widely used Santa Barbara DISORT Atmospheric Radiative Transfer (SBDART) model—a detailed description of which may be found in Ricchiazzi and Yang (1998). The important input parameters include aerosol optical depth (AOD), light extinction coefficient (b_{scat}+b_{abs}), SSA, asymmetric parameter (ASP), and visibility. Here, the input optical parameters were estimated by Optical Property of Aerosol and Cloud (OPAC) model using Mie theory (Hess et al., 1998). The measured BC, water-soluble matter (including measured water-soluble inorganic ions and water-soluble organic matter that assumes accounting for 79% of OC loading, Xu et al., 2015), and water insoluble matter (calculated as the $PM_{2.5}$ mass concertation minus those of BC and water-soluble matter) were used in the OPAC model to retrieve the number concentrations of these particles. These were tuned untill the modelled $b_{scat}(\lambda)$, $b_{abs}(\lambda)$, SSA were within ±5% (Srivastava et al., 2012) of the values measured by PAX (see Table S1) and used to obtain the optical parameters at the nearest observed relative humidity. The underlying assumption was that when the modelled $b_{scat}(\lambda)$, $b_{abs}(\lambda)$ were very close to their measured counterparts, the derived optical parameters were a reasonable representation of the measured aerosols. This assumption has been widely used in previous studies (Dumka et al., 2018; Panicker et al., 2010; Rajesh et al., 2018). Finally, the DREs attributable to source-specific BC (or $PM_{2.5}$) at the surface atmosphere (SUF) and the top of the atmosphere (TOA) were estimated as the difference in the net flux with and without BC (or $PM_{2.5}$) under cloud-free conditions. The solar heating rate change induced by atmospheric DRE (DRE at TOA subtracts DRE at SUF) was calculated as follows (Ramachandran and Kedia, 2010):

$$DRE_{ATM} = DRE_{TOP} - DRE_{SUF} \quad (11)$$

$$\frac{\partial T}{\partial t} = \frac{g}{C_p} \times \frac{DRE_{ATM}}{\Delta P} \quad (12)$$

移动了(插入) [1]

删除了: spatial resolution

删除了: was used in model,

删除了: ding

删除了: , which was

上移了 [1]: based on the Asian anthropogenic emission inventory (that is MIX) for the year of 2010 (Li et al., 2017).

删除了: forcing

删除了: forcing

删除了: F

删除了: as

删除了: by

删除了: . The

删除了: SBDART model

删除了: is elaborated

删除了: ,

删除了: These aerosol

删除了: on the TP

删除了: by

删除了: of $PM_{2.5}$

删除了: matters

删除了: which were then further used to obtain the optical parameters at the nearest observed relative humidity.

删除了: number concentrations

删除了: close to the ones measured by PAX, with a difference within ±5% (Srivastava et al., 2012) (see Table S1)

删除了: is

删除了: are

删除了: rest

删除了: are assumed

删除了: for

删除了: accepted

删除了: F

删除了: induced by

删除了: alone

删除了: by

删除了:

删除了: Atmospheric forcing

删除了: F

删除了: F

删除了: leads to solar heating rate change, which can be

where DRE_{ATM} (W m^{-2}) is the atmospheric DRE; DRE_{TOP} is the DRE at top atmosphere; DRE_{SUF} is the DRE at surface atmosphere; $\frac{\partial T}{\partial t}$ is the heating rate (K day^{-1}); g is the acceleration due to gravity (9.8 m s^{-2}); C_p is the specific heat capacity of air at constant pressure; and ΔP is the difference in atmospheric pressure between the ground and 3 km above.

3 Results and discussion

3.1 Source-dependent AAEs and MACs

Four sources were identified as the main contributors to primary $b_{abs}(\lambda)$ based on the optical source apportionment (Fig. 2). The simulated primary b_{abs} (λ) values at different wavelengths all correlated well ($r = 0.96 – 0.97$, $p < 0.01$, Fig. S1) with the model inputs, indicating that the PMF5.0 performed well. As shown in Fig. 2, the first source factor exhibited high contributions of K^+ (90%), levoglucosan (60%), and primary $b_{abs}(\lambda)$ (45 – 64%) as well as moderate loadings of OC (38%) and EC (47%). The K^+ and levoglucosan are widely used markers for biomass burning (Urban et al., 2012), and these chemical markers are strong indications that this factor resulted from biomass burning emissions. Furthermore, we note that the presence of BrC in this factor made higher absorption at shorter wavelengths, which is consistent with absorption feature of biomass burning emissions (Forello et al., 2019). Based on the contributions of biomass burning to $b_{abs}(370)$ and $b_{abs}(880)$, the $AAE_{biomass}$ was estimated to be 1.7, which is within a relative boarder range of $AAE_{biomass}$ (1.2 – 3.5) determined by other methods (e.g., $\Delta^{14}C$ and organic tracers) in previous studies (Sandradewi et al., 2008; Helin et al., 2018; Harrison et al., 2012; Zotter et al., 2017). The estimated average $MAC_{BC}(880)_{biomass}$ was 10.4 m^2 g^{-1}; this is more than twice the value for uncoated BC particles suggested by Bond and Bergstrom (2006) ($MAC_{BC}(880)_{uncoated}$ = 4.7 m^2 g^{-1}, extrapolated from 550nm to 880 nm by assuming AAE_{BC} = 1.0). The large $MAC_{BC}(880)$ indicates that BC particles from biomass burning experienced substantial aging processes during their transport because numerous studies have confirmed that aged BC could result in MAC increases by a factor of 1.5–3.5 relative to uncoated particles (Chen et al., 2017; Ma et al., 2020) due to the 'lensing effect' (Lack and Cappa, 2010).

删除了: ,
删除了: ΔF_{ATM} is the atmospheric forcing;
删除了: Based on the optical source apportionment, four sources were identified contributing to primary $b_{abs}(\lambda)$ (Fig. 1)
删除了: 2
删除了: those
删除了: values
删除了: a good reproducibility of
删除了: 1
删除了: .
删除了: Owing to
删除了: , the
删除了: fraction increased toward to
删除了: the optical
删除了: Therefore, this source factor was assigned to biomass burning. …
删除了: reported by previous studies obtained via comparison with other measurements
删除了: the atmosphere
删除了: ,
删除了: which was
删除了: over
删除了: two times
删除了: larger than the value of
删除了: ,
删除了: This indicates
删除了: -
删除了: -related
删除了: BC particles
删除了: . The enhancement in $MAC_{BC}(880)_{biomass}$ can be explained by …
删除了: due to the BC particles internally-mixed with other substances …

The second source factor was characterized by large loadings of benzothiazolone (54%), Pb (46%), Br (40%), Cu (35%), Zn (27%), EC (36%), and OC (30%). Benzothiazolone is released from the breakdown of the antioxidant in motor vehicle tires (Cheng et al., 2006) while Br is another tracer of motor vehicle emission (Guo et al., 2009). Similarly, Zn and Cu are associated with the combustion of lubricating fluids and the wear of brakes and tires (Lough et al., 2005; Song et al., 2006). Finally, EC and OC also are components of motor vehicle emissions (Cao et al., 2013). Although unleaded gasoline has been used extensively used in China since 2005, a considerable portion of Pb in the environment is still associated with vehicle-related particles, especially from the wear of metal alloys (Hao et al., 2019). Therefore, this second source factor was identified as traffic-related emissions. This source constitutes a moderate percentage of primary $b_{abs}(\lambda)$ (15–30%). The estimated traffic emission-related AAE ($AAE_{traffic}$) was 0.8, consistent with the finding that BC is the dominant light-absorbing carbonaceous aerosol species for traffic emissions (Kirchstetter et al., 2004). The $AAE_{traffic}$ found here also was close to a value obtained using the $\Delta^{14}C$ approach (Zotter et al., 2017). The estimated $MAC_{BC}(880)$ of traffic emissions ($MAC_{BC}(880)_{traffic}$ = 9.1 m^2 g^{-1}) was similar with $MAC_{BC}(880)_{biomass}$, indicating that traffic emission-related BC particles were also subjected to substantial aging.

The third factor was dominated by high loadings of As (70%), S (37%), and Cu (47%), which are typically associated with coal combustion (Hsu et al., 2016; Kim and Hopke, 2008). Although coal is not used extensively near the site on the TP, emissions from coal combustion may have been transported to site from surrounding areas (e.g., East Asia, Li et al., 2016). This source contributed 12–17% of primary $b_{abs}(\lambda)$, which is less than that from biomass burning or traffic emissions. The obtained AAE of coal combustion (AAE_{coal} = 1.1) was similar to the $AAE_{traffic}$, suggesting that BC was also the dominant light-absorbing carbon specie in coal combustion emissions. The AAE_{coal} was close to the value of chunk coal combustion (1.3) but lower than that for briquettes coal (2.6) (Sun et al., 2017) ; this presumably reflects the types of coal transported to Gaomeigu, at least to some degree. The estimated BC MAC(880) of coal combustion ($MAC_{BC}(880)_{coal}$ = 15.5 m^2 g^{-1}) was larger than $MAC_{BC}(880)_{biomass}$ and $MAC_{BC}(880)_{traffic}$. The enhance factor for $MAC_{BC}(880)_{coal}$ (3.3) falls near the upper limit of this range noted above, and although this is likely related to the aging of BC particles during transport to Gaomeigu, more work is need to verify this contention in future studies.

删除了： The…Bb…nzothiazolone is a substance …eleased from the breaking-…own of the antioxidant in motor vehiclevehicular…tires (Cheng et al., 2006) while.…Br is anothera…tracer of closely related to …otor vehicle emission (Guo et al., 2009). Similarly,, and…Zn and Cu are associated with the combustion of lubricating fluids and the wearing…of brakes and tires (Lough et al., 2005; Song et al., 2006). FinallyMeanwhile… EC and OC also are can be …omponents ofused to denote…motor vehicle emissions (Cao et al., 2013). Although unleaded gasoline has been used extensively used in China since 2005, a considerable portion of Pb in the environment is still associated with found in …ehicle-related particles, especially from which may be relation with…the wear of metal alloys (Hao et al., 2019). Therefore, this second source factor was identified as traffic-related emissions. This source constitutes a moderate percentage of primary $b_{abs}(\lambda)$ (15–30%). The estimated traffic emission-related AAE ($AAE_{traffic}$) was 0.8, consistent with the findingfeature…that BC is the dominant light-absorbing carbonaceous aerosol speciescarbon…for traffic emissions (Kirchstetter et al., 2004). The $AAE_{traffic}$ found here is …lso was close to a value obtained using thethose obtained with…$\Delta^{14}C$ approach (Zotter et al., 2017). The estimated BC …

设置了格式： 下标

删除了： is a…typically associated withfeature of…coal combustion (Hsu et al., 2016; Kim and Hopke, 2008). Although coal is nota…usedscarce…extensively near the site energy used …n the TP, emissions from it can be influenced by…coal combustion may have been transported to site from surrounding areas (e.g., East Asia, Li et al., 2016). This source contributed only …2–17% of primary $b_{abs}(\lambda)$, which is less than that from biomass burning or and …raffic emissions. The obtained AAE of coal combustion (AAE_{coal} = 1.1) was similar to the $AAE_{traffic}$, suggesting that BC was also thea…dominant light-absorbing carbon specie in coal combustion emissions. The AAE_{coal} wasis…close to the value of chunk coal combustion (1.3) but lower than that for to …

删除了： , which may …eflects the coal …ypes of coal transported to that affected BC particles at …aomeigu, at least to some degree. The estimated BC MAC(880) of coal combustion ($MAC_{BC}(880)_{coal}$ = 15.5 m^2 g^{-1}) was larger than $MAC_{BC}(880)_{biomass}$ and $MAC_{BC}(880)_{traffic}$. Numerous studies have confirmed that aged BC could result in MAC increased by a factor of 1.5 – 3.5 relative to uncoated one (Chen et al., 2017; Ma et al., 2020). …he enhance factor for $MAC_{BC}(880)_{coal}$ (3.3) falls near the upper limit of this range noted above,…and although tT…is is likely large enhancement should be …elated to the aging processes …f BC particles during their long-range …ransport Gaomeigu, although…more work is need to verify this contention in future studiesexplain in the future …

The fourth source factor had high loadings of Ca (35%), Ti (66%), Mn (47%), and Fe (61%), consistent with the characteristics of crustal elements (Guo et al., 2009); thus, it was assigned to soil dust. The light absorption of soil dust is mainly due to the presence of iron oxides and varies with the types and relative concentrations of iron oxide species (Alfaro, 2004; Valenzuela et al., 2015). The mineral dust here contributed a relative small amount to the primary $b_{abs}(\lambda)$ (6–9%), presumably due to the low levels of iron oxides, and this is consistent with the other results obtained on the southeastern TP (Zhao et al., 2019). The estimated AAE of mineral dust (AAE_{dust}) was 1.5, which is within the range of 1.2–3.0 obtained from multi-non-oceanic sites (Dubovik et al., 2002).

3.2 BC source apportionment

As the results above showed that fossil fuel-related BC aerosol mainly originated from traffic and coal combustion, the AAE_{fossil} (0.9) and $MAC_{BC}(880)_{fossil}$ (12.3 m^2 g^{-1}) were averaged by the values of $AAE_{traffic}$ + AAE_{coal} and $MAC_{BC}(880)_{traffic}$ + $MAC_{BC}(880)_{coal}$, respectively as shown in Table 1. Based on the source-specific AAEs (i.e., AAE_{fossil} and $AAE_{biomass}$) and BC $MAC_{BC}(880)$ (i.e., $MAC_{BC}(880)_{fossil}$ and $MAC_{BC}(880)_{biomass}$), the mass concentrations of BC_{fossil} and $BC_{biomass}$ were then estimated using the improved 'aethalometer model' (Eqs. 1– 6). As shown in Fig. 3a, no correlation ($r = 0.01$, $p = 0.02$) was found between $BC_{biomass}$ and BC_{fossil}, implying that BC from these two sources was effectively separated by the improved aethalometer model. The data for the biomass-burning and traffic-related tracers (levoglucosan and benzothiazolone, respectively) further support the results of BC source apportionment. That is, $BC_{biomass}$ was significantly correlated with levoglucosan ($r = 0.75$, $p < 0.01$, Fig. 3b) and the same was true for BC_{fossil} benzothiazolone ($r = 0.67$, $p < 0.01$, Fig. 3c), respectively. These results indicate that the source-specific AAEs and MACs(880) obtained from optical source apportionment were appropriate. Fig. 3d shows a time series plot of hourly averaged mass concentrations of total BC, $BC_{biomass}$, and BC_{fossil} during the campaign. The hourly total BC mass concentration varied by ~50-fold from 0.1 to 4.9 μg m^{-3}, with an arithmetic mean (± standard deviation) of 0.7 (± 0.5) μg m^{-3}, which was lower than what has been reported for the western TP but higher than in the northern TP (Wang et al., 2018, and references therein). The larger BC loading in the western TP can be explained by relatively strong influences from Southeast Asia, where anthropogenic actives are intensive (Kurokawa et al., 2013). With reference to BC sources,

删除了: was enriched of
删除了: .
删除了: T
删除了: diversity of iron
删除了: contents
删除了: minor to
删除了: content
删除了: which was
删除了: nvolves BC emitted
删除了: (1)
删除了: (7)
删除了: S
删除了: can be
删除了: reasonably
删除了: tracer
删除了: (levoglucosan)
删除了: were used to
删除了: verify
删除了: As expected
删除了: and BC_{fossil} correlated
删除了: S
删除了: S
删除了: for the improved 'aethalometer model'.
删除了: 2
删除了: the
删除了: almost
删除了: those in the
删除了: is mainly attributed to the influences of
删除了: In terms of different

the concentrations and contributions as listed in Table 1, show higher mass concentrations of $BC_{biomass}$ (0.4 ± 0.3 μg m^{-3}, 57% of total BC) compared with BC_{fossil} (0.3 ± 0.2 μg m^{-3}, 43% of total BC) on average. The mass fraction of $BC_{biomass}$ increased with the BC loadings while BC_{fossil} mass fraction showed an inverse relationship to the loadings (Fig. S2). One can infer from this that biomass-burning emissions were responsible for the high BC loading episode during the campaign.

Distinct diurnal variations in the mass concentrations of $BC_{biomass}$ and BC_{fossil} were observed as shown in Fig. 4a. The $BC_{biomass}$ started to increase after midnight, reached a small peak at ~05:00 and then remained at a constant level before sunrise (~08:00). This may be attributed to effects associated with changes in the height of the planetary boundary layer (PBL) height (https://rda.ucar.edu/datasets/ds083.2) (Fig. 4b). Thereafter, the $BC_{biomass}$ increased again and reached the maximum value at midday. This enhancement was accompanied by an increase in PBL height and higher wind speed (https://rda.ucar.edu/datasets/ds083.2) (Fig. 4b). Generally, higher PBLs and stronger wind cause local pollutants to disperse and as a result lower their loadings (Wang et al., 2015). However, thus the build up of $BC_{biomass}$ in daytime at Gaomeigu was more likely influenced by the transport of $BC_{biomass}$ from regions upwind. After sunrise, the PBL began to deepen and that was accompanied with west/southwest winds from 08:00 to 12:00 (Fig. S3). These meteorological conditions are favourable for pollutants (including BC) transport from high-density biomass-burning emission areas to the sampling site (Chan et al., 2017). After the midday peak, $BC_{biomass}$ decreased sharply until midnight. The initial portion of this decrease (13:00 – 18:00) occurred as the PBL height and wind speed increased, which promoted the dispersion of $BC_{biomass}$. Subsequent reduction occurred at night even though the PBL height and wind speed decreased, and that was likely due to the curtailment of local biomass-burning activities.

As shown in Fig. 4a, the BC_{fossil} showed diurnal trend that was roughly opposite trend that of the unimodal pattern seen for $BC_{biomass}$, and that may be explained as follows. Increases in the PBL height and wind speed from 09:00 to 15:00 were associated with a decrease in BC_{fossil}, unlike the increasing trend seen for $BC_{biomass}$; this presumably reflects minor effects from the regional transport on BC_{fossil}. Further, because of the small contribution of coal combustion to EC (12%, Fig. 2c), the BC_{fossil} was best explained by motor vehicle emissions from areas upwind of the site. The subsequent increase in BC_{fossil} from 17:00 to 20:00 was attributed to the reduction of PBL height and as a result the build up of pollutants in the near

删除了: mass …oncentrations and contributions as listed in Table 1, show higher mass concentrations of $BC_{biomass}$ (0.4 ± 0.3 μg m^{-3}, 57% of total BC) compared withwas slightly higher than…BC_{fossil} (0.3 ± 0.2 μg m^{-3}, 43% of total BC) on average. The mass fraction of $BC_{biomass}$ increased withenhanced as…the BC loadings increased …hile BC_{fossil} mass fraction showed an inverse relationship to the loadings (Fig. S2) trend (Fig. S4)… One can infer from this thatThis suggests and …

删除了: (Fig. 3a)… TheFor…$BC_{biomass}$, it…started to increase after midnight, reachedmidnight reaching…a small peak at ~05:00 and then remained at a constant level before sunrise (~08:00). This may be attributed to effects associated with changes in the height of the This may be attributed to the accumulative effect caused boundary layer (PBL) height (https://rda.ucar.edu/datasets/ds083.2), which showed a declining trend during this period…(Fig. 43…). Thereafter, the $BC_{biomass}$ increased again and reached the maximum value of the day …t midday. This enhancement was accompanied by an the …ncrease ind…PBL height and higher wind speed (https://rda.ucar.edu/datasets/ds083.2) (Fig. 43…). Generally, higherdeeper…PBLs and stronger winds…cause accelerate …ocal pollutants to disperse diffusion…and as a result lower their loadings (Wang et al., 2015). However, thus the build up the increased trend here was more likely influenced by regional transport …f $BC_{biomass}$ in daytime at Gaomeigu was more likely influenced by the transport of $BC_{biomass}$ from regions upwind region… After sunrise, the PBL height …egan to deepenrise…and that was accompanied with west/southwest winds from 08:00 to 12:00 (Fig. S35…. These favourable …eteorological conditions are favourable provided good transport advantages …or pollutants (including BC) transport from high-density biomass-burning emission areas to the sampling site (Chan et al., 2017). After the midday peak, $BC_{biomass}$ decreased sharply until midnight. The initial portion of this decrease (13:00 – 18:00) occurred aswas mainly attributed to the continuous…the increases in …BL height and wind speed increased, which promoted the dispersion of $BC_{biomass}$ diffusion… SubsequentThe further…reduction occurred at night was due to the scarcity of local biomass-burning activities, …ven al …

删除了: during this period.
As shown in Fig. 43…, different from the unimodal diurnal pattern of $BC_{biomass}$, …he BC_{fossil} showed diurnal trend that wasa…roughly opposite trend that of the unimodal pattern seen for $BC_{biomass}$,….and that may be explained as follows. IOwing to the influence of diffusion effect caused by i…creases in the PBL height and wind speed , BC_{fossil} decreased …rom 09:00 to 15:00 were associated with a decrease in BC_{fossil}, unlike the increasing trend seen for $BC_{biomass}$;….this presumably reflects The initial morning decrease in BC_{fossil} was just opposite to the increasing trend of $BC_{biomass}$, reflecting …inor effects from the regional transport contributing to …n BC_{fossil}. Further, because of the small contribution of coal combustion to EC (12%, Fig. 21…), the BC_{fossil} was best explainedmainly contributed…by motor vehicle emissions from areas upwind of the sitethe surrounding areas of southeastern TP… The subsequent increase in BC_{fossil} from 17:00 to 20:00 was attributed to the reduction of PBL height and as a result the build up ofaccumulated… …

surface air. As there were minimal impacts from traffic at night, the BC_{fossil} loadings remained steady from 21:00 to 08:00. The stable nocturnal BC_{fossil} may reflect the impact of fossil fuel emissions on BC in the southeastern margin of the TP due to the accumulation resulting from the low PBL heights.

3.3 Regional influences of $BC_{biomass}$ and BC_{fossil}

To investigate the regional impacts on BC, three groups of air masses were identified based on their transport pathways (Fig. 5a). Cluster 1 originated from northeastern India and then passed over Bangladesh before arriving Gaomeigu. The average BC mass concentration of this cluster was the highest (0.8 ± 0.4 μg m^{-3}) of the three clusters. About 74% of total trajectories were associated with Cluster 1, of which 22% was identified as polluted and had an average BC loading of 1.3 ± 0.5 μg m^{-3}. Cluster 2 originated over Burma had an average BC loading of 0.7 ± 0.7 μg m^{-3}. This cluster c accounted for only 24% of total trajectories, but among them, about 37% was referred to pollution with BC reaching as high as 1.6 ± 0.9 μg m^{-3}. The air masses associated with Cluster 3 originated from the interior of China, and this group had the lowest BC mass concentrations of the three clusters, 0.4 ± 0.1 μg m^{-3}. This third cluster composed small fraction of total trajectories (2%), and none of them were identified as polluted, suggesting minor influences from the mainland China during the campaign.

The diurnal patterns of $BC_{biomass}$ and BC_{fossil} mass loadings from the three clusters were used to investigate the impacts of regional transport. As shown in Fig. 4c and e, similar diurnal variations in $BC_{biomass}$ were found for Clusters 1 and 2—they had both larger values during daytime (8:00–12:00) compared with night. This pattern of higher daytime $BC_{biomass}$ was associated with regional transport from northeastern India (Cluster 1) and Burma (Cluster 2). For Cluster 3, $BC_{biomass}$ decreased during the day and increased at night (Fig. 4g), and that pattern tracked the daily variations in PBL height. Unlike Clusters 1 and 2, the diurnal variation of $BC_{biomass}$ for Cluster 3 were more likely due to influences of biomass-burning activities from areas surrounding the sampling site than regional transport. However, it should be noted that these cases were uncommon because of only 2% of air-masses were associated with Cluster3.

For BC_{fossil}, similar diurnal patterns were found for Clusters 1 and 2 (Fig. 4c and e), most likely due to the influences of traffic emissions from surrounding areas as well as daily cycles of PBL height as discussed in section 3.2. The BC_{fossil} loadings of Cluster 3 (Fig.4g) were relatively stable, showing only

删除了: the southeastern TP… AsSince…there were s…minimal impacts fromcarce…traffic activities …t night, the BC_{fossil} loadings remained at a…steady concentration …rom 21:00 to 08:00. The stable nocturnal BC_{fossil} may reflect the impact of fossil fuel emissions on BC in the southeastern margin of the TP due to the accumulation resulting from effect driven by …

删除了: 4…). Cluster #… originated from northeastern India and then passed over Bangladesh before arriving Gaomeigu. The average BC mass concentration of this cluster was the highest (0.8 ± 0.4 μg m^{-3}) of among …he three clusters. About 74% of total trajectories were associated with Cluster #…, of which 22% was identified as polluted and had ones with …n average BC loading of 1.3 ± 0.5 μg m^{-3}. Cluster #… originated overderived from…Burma hadwith…an average BC loading of 0.7 ± 0.7 μg m^{-3}. This cluster c accounted foronstituted…only 24% of total trajectories, but among them, about 37% was referred to pollution with BC reaching as high as 1.6 ± 0.9 μg m^{-3}. The air masses associated with Cluster #… originated from the interior of mainland…China, and which…this group had the lowest BC mass concentrations of the three clusters,of…0.4 ± 0.1 μg m^{-3}. This third cluster composedcomprised…small fraction of total trajectories (2%), and none of them wereas…identified as pollutedpollution… …

删除了: different…clusters were further …sed to investigate the impacts of regional transport. As shown in Fig. 43… and e, a …imilar diurnal variations of …n $BC_{biomass}$ was …ere found for Clusters #… and Cluster…#…—, …hey had bothwith…larger values during daytime (8:00–12:00) compared with the …ight-time… This pattern of higher daytime $BC_{biomass}$ was associated withThe enhancements of daytime $BC_{biomass}$ (8:00 – 12:00) were related to…the …egional transport from northeastern India (Cluster #…) and Burma (Cluster #…). For Cluster #…, the diurnal variation of…$BC_{biomass}$ decreased during the daytime…and increased at night (Fig. 43…), and that pattern trackedwhich was mainly controlled by…the daily variationsvariability…in PBL height. Unlike Clusters 1 and 2,Compared to other two clusters,…the inverse …iurnal variation of $BC_{biomass}$ for Cluster #… were more likely due toindicates the…influences of biomass-burning activities from areasthe…surrounding the sampling site areas rather …han regional transport. However, it should be noted that these cases were uncommonscarce…because of only 2% of air-masses were associated with Cluster # …

删除了: a …imilar diurnal patterns was …ere found for Clusters #… and Cluster #… (Fig. 43… and e), most likely due to which was mainly associated with …he influences of traffic emissions from in…surrounding areas as well as daily cycles of PBL height as discussed in section 3.2. The BC_{fossil} loadings of Cluster #… (Fig.3g…g) wereexhibited a …

sporadic fluctuations. Unlike the declining trend of BC_{fossil} during the daytime found for Clusters 1 and 2, the relative stable BC_{fossil} loadings in Cluster 3 indicate that there were emissions from fossil fuel sources that offset the effect of the changes in PBL height. The transportation sector has grown rapidly in mainland China (Liu, 2019), and the regional transport of motor vehicle emissions may have been the cause for the observed diurnal variations in BC_{fossil} for Cluster 3.

The PSCF model was applied to further investigate the likely spatial distribution of pollution source regions for $BC_{biomass}$ and BC_{fossil}. As shown in Fig. 5b, a low PSCF value of $BC_{biomass}$ was found near Gaomeigu while high values were concentrated in the northeastern India and northern Burma, consistent with intensive fire activities in these areas (Fig. S4). This indicates that large $BC_{biomass}$ loadings at Gaomeigu were more likely influenced by cross-border transport of biomass burning rather than local emissions. For BC_{fossil} (Fig. 5c), the most likely impact region was located to the southweast of Gaomeigu, near where two highways are located (e.g., Hangzhou-Ruili Expressway and Dali-Nujiang Expressway). Owing to the low consumption of coal in the southeastern TP (Li et al., 2016), the high PSCF values of BC_{fossil} were more likely from traffic emissions than coal combustion. Moreover, sporadic high PSCF values of BC_{fossil} also were found in the northern Burma, indicating possible influences of fossil fuel emissions here.

To further quantify the contributions of the BC transported from Southeast Asia to Gaomeigu, we studied a high BC episode (23 – 27 March) using a simulation with WRF-Chem model. Two scenarios of emissions were simulated: one involved all BC emission sources, and the other turned off biomass-burning emissions in Southeast Asia. The variation of modelled BC mass concentration shows an acceptable degree of consistency with the measured values ($r = 0.63$, $p < 0.01$, Fig. S5). Furthermore, the index of agreement was estimated to be 0.77, indicating that the development of this BC episode was effectively captured by the WRF-Chem model. Nonetheless, the normalized mean bias between the measured and modelled BC values was estimated to be 24%, suggesting that simulation was biased towards high values. This discrepancy is best attributed to the uncertainties in the simulation associated with the emission inventory and meteorological conditions. Fig. 6a shows the spatial distributions of BC loadings in Gaomeigu and surrounding areas. The mass concentrations of BC at times exceeded 15 μg m^{-3} over Burma and northern India, and that is more than an order of magnitude higher compared with the

删除了: diurnal variation expect for …poradic fluctuations. Unlike the declining trend of BC_{fossil} during the daytime found for Clusters 1 and 2in the other two clusters… the relative stable BC_{fossil} loadings variation…in Cluster #… indicates…that there were emissions from fossil fuel sources that to …ffset the effect of the changes inpollutant diffusion caused by increased…PBL height. The transportation sector has grown rapidlyOwing to the high-density transportation network…in mainland China (Liu, 2019), and the regional transport of motor vehicletraffic…emissions may have been the cause for the observed diurnal variations in BC_{fossil} for Cluster 3be the cause …

删除了: Further,… t…e PSCF model was applied to further investigate the likely spatial distribution of pollution source regions for $BC_{biomass}$ and BC_{fossil}. As shown in Fig. 54…, a low PSCF value of $BC_{biomass}$ was found near Gaomeigu while high values were concentrated in the northeastern India and northern Burma, consistent with intensive fire activitiesspots…in these areas (Fig. S46…. This indicates that large $BC_{biomass}$ loadings at Gaomeigu were more likely influenced by cross-border transport of biomass burning rather than local emissions. For BC_{fossil} (Fig. 54…), the most likelypossible…impact region was located to near …he southweast of Gaomeigu, near where two highways are locatedthere are a few villages scattered around and two highways…(e.g., Hangzhou-Ruili Expressway and Dali-Nujiang Expressway). Owing to the low consumption of coal in the southeastern TP (Li et al., 2016), the high PSCF values of BC_{fossil} were more likely frommay be mainly contributed by…traffic emissions rather …han coal combustion. Moreover, sporadic high PSCF values of BC_{fossil} also were also …

删除了: transported…to BC at …aomeigu, we studied a high BC episode (23 – 27 March) using a simulationwas arbitrary selected and…withsimulated by the …

删除了: one …r = 0.63, $p < 0.01$, Fig. S57…, Furthermore, and …he index of agreement was estimated to be 0.77, indicating that the development formation process…of this BC episode was effectively captured by the WRF-Chem model. NonethelessHowever… it should be noted that …he normalized mean bias between the measured and modelled BC values was estimated to be 24%, suggesting that simulation was biased towards high valuesan overestimation of simulation… This discrepancy is best attributedcould be attributed…to the simulation …

删除了: resulted from…the emission inventory and meteorological conditions. Fig. 65… shows the spatial distributions of BC loadings in Gaomeigu and surrounding areas. The mass concentrations of BC at timescan…exceeded 15 μg m^{-3} overin…Burma and northern India, and that iswhich was…more thanover…one …n order of magnitude higher compared withthan that in …

southeastern margin of TP (0.7 μg m^{-3}). After turning off the biomass burning emission source in Southeast Asia, the BC loading at southeastern TP dropped over 40% (Fig. 6b), suggesting a substantial impact of biomass-burning activities in Southeast Asia countries, which is consistent with results of the trajectory cluster analysis and PSCF.

3.4 Radiative effects and heating rate

Fig. 7 shows the average atmospheric direct radiative effects of $PM_{2.5}$ and BC (including $BC_{biomass}$ and BC_{fossil}) at the TOA and SUF during the campaign. The average $PM_{2.5}$ DRE at the TOA was +0.03 ± 1.1 W m^{-2}, implying that the positive effect of light-absorbing carbon on the temperature of the atmosphere outweighed the negative effect of scattering aerosols. In fact, BC produced +1.6 ± 0.8 W m^{-2} at the TOA on average. At the SUF, BC DRE (-3.0 ± 1.5 W m^{-2}) contributed nearly half of the $PM_{2.5}$ DRE (-6.3 ± 4.5 W m^{-2}). The difference in the DRE between the TOA and SUF was +4.6 ± 2.4 W m^{-2} for BC aerosol, and that accounted for 73% of DRE attributed to $PM_{2.5}$ (6.3 ± 4 W m^{-2}), this suggests substantial radiative effect caused by BC over the southeastern margin of TP even though its mass fraction is small in $PM_{2.5}$ (3.3%).

With respect to the BC sources (Fig. 7), the average $BC_{biomass}$ (BC_{fossil}) DRE was +0.8 ± 0.6 W m^{-2} (+0.7 ± 0.4 W m^{-2}) at the TOA, and -1.7 ± 1.2 W m^{-2} (-1.4 ± 0.6 W m^{-2}) at the SUF. This is equivalent to an average atmospheric DRE of +2.5 ± 1.8 W m^{-2} (+2.1 ± 0.9 W m^{-2}). Presumably, the influences of regional transport caused the atmospheric DRE of $BC_{biomass}$ to be more variable compared with that from BC_{fossil} (Fig. S6). For example, the atmospheric DRE of $BC_{biomass}$ can be as high as +6.4 W m^{-2} when the air masses passed over the biomass-burning regions in Southeast Asia, while it was only 1.1 ± 0.2 W m^{-2} on average when the air masses passed from the mainland of China.

The calculations showing a positive atmospheric DRE imply that energy was trapped in the atmosphere, which would lead to atmospheric heating over the study region. The heating rate calculated for BC varied from 0.02 to 0.3 K day^{-1} and an average of 0.13 ± 0.07 K day^{-1}. In terms of the DRE efficiency, the heating rate caused by a unit mass concentration of BC in this region was (0.19 (K day^{-1}) (μg m^{-3})$^{-1}$), which is roughly comparable with that reported for Qinghai Lake, on the northeastern TP (0.13 (K day^{-1}) (μg m^{-3})$^{-1}$) (Wang et al., 2015), but it generally lower than the values in the southwestern regions of the Himalaya

删除了: 5…), suggesting a substantial impact of biomass-burning activities in Southeast Asia countries, on BC at the sampling site, …hich is was …onsistent with results of the trajectory cluster analysis and PSCF results …

删除了: forcing

删除了: 6…shows the average atmospheric direct radiative effectsDRFs…of $PM_{2.5}$ and BC (including $BC_{biomass}$ and BC_{fossil}) at the TOA and SUF during the campaign. The average DRF of…$PM_{2.5}$ DRE at the TOA was +0.03 ± 1.1 W m^{-2}, implying that the positive effect ofthe importance of…light-absorbing carbon on the of the atmosphere outweighed the negative effect of scattering aerosols. In factActually… the …C can …roduced +1.6 ± 0.8 W m^{-2} at the TOA on average. At the SUF, BC DREforcing…(-3.0 ± 1.5 W m^{-2}) contributeds…nearly half of the $PM_{2.5}$ DREforcing…(-6.3 ± 4.5 W m^{-2}). The difference in the DRE between the TOA and SUFnet forcing trapped in the atmosphere…was +4.6 ± 2.4 W m^{-2} for BC aerosol, and that accounted forwhich comprised…73% of DRE attributed tothat caused by…$PM_{2.5}$ (6.3 ± 4 W m^{-2}), this suggeststsuggesting a…substantial radiative effect caused by BC overin…the southeastern margin of TP even though, although …

设置了格式: 字体: Times New Roman

删除了: From the perspective of…the BC sources (Fig. 76…, the average $BC_{biomass}$ (BC_{fossil}) DREF…was +0.8 ± 0.6 W m^{-2} (+0.7 ± 0.4 W m^{-2}) at the TOA, and -1.7 ± 1.2 W m^{-2} (-1.4 ± 0.6 W m^{-2}) at the SUF. This is equivalent tocauses…an average atmospheric DREradiative forcing…of +2.5 ± 1.8 W m^{-2} (+2.1 ± 0.9 W m^{-2}). Presumably, the influences ofOwing to the impacts of…regional transport , …aused the atmospheric DRE forcing …f $BC_{biomass}$ to be more variable compared with that fromwas more fluctuation relative to… …

删除了: 8…. For example, the average …tmospheric DREforcing…of $BC_{biomass}$ can bereach…as high as +6.45.6…W m^{-2} when t…hehe coming…air masses passed over the biomass-burning regions in Southeast Asia, while it was only 1.1 ± 0.2 W m^{-2} on average when the air masses passed from the mainland of China.. …

删除了: forcing…imply thatindicates the trapping of…energy was trapped in the atmosphere, which would leadleading…to an increase in …tmospheric heating over the study regionin the southeastern margin of TP… The heating rate calculated for caused by …C varied from 0.02 to 0.3 K day^{-1} andwith…an average of 0.13 ± 0.07 K day^{-1}. In terms of the DREF…efficiency, the heating rate caused by a unit BC …ass concentration of BC in this region was is found higher …

删除了: ed…with that in …eported for Qinghai Lake, on the northeastern TP (0.13 (K day^{-1}) (μg m^{-3})$^{-1}$) (Wang et al., 2015), but it was…generally lower than the values in the southwestern regionssouthwest …

(Fig. S7). Moreover, the heating rate caused by $BC_{biomass}$ may have been slightly higher (0.07 ± 0.05 K day^{-1}) compared with BC_{fossil} (0.06 ± 0.02 K day^{-1}). Finally, the heating rate of $BC_{biomass}$ increased to 0.16 K day^{-1} when the BC mass concentration was heavily influenced by the polluted air from Southeast Asia.

4 Conclusions

This study quantified the source contributions of BC aerosol from fossil fuel and biomass burning at a site on the southeastern margin of the TP that represents a regional transport channel for air pollution during pre-monsoon. The study was conducted in pre-monsoon when the southeastern TP was heavily influenced by the air mass from southeast Asia. To reduce the uncertainties caused by interferences in absorption measurements (i.e. secondary absorption and dust) and assumptions relative to AAEs and MAC_{BC}s, the traditional 'aethalometer model' was optimized in two aspects. First, a BC-tracer method coupled with a minimum R-squared approach was applied to separate secondary absorption from the total absorption, and as a result, the interferences of absorption from secondary aerosols have been eliminated. Then, an optical source apportionment model that used primary multi-wavelength absorption and chemical species as inputs was used to derive site-dependent AAE and MAC_{BC} values—these minimize the uncertainties associated with prior assumptions on these parameters. The AAE (MAC_{BC}) calculated in this way was 0.9 (12.3 m^2 g^{-1}) for fossil fuel source and 1.7 (10.4 m^2 g^{-1}) for biomass burning. The results of 'aethalometer model' that used these values showed that the average mass concentration of BC was 0.7 ± 0.5 μg m^{-3} of which 43% of BC from fossil fuel and 57% from biomass burning. Trajectory analysis showed that the $BC_{biomass}$ over the site was mainly driven by regional transport from northeastern India and Burma, while BC_{fossil} was primarily influenced by traffic emissions from areas surrounding the sampling site. Moreover, the WRF-Chem model indicates that biomass burning in Southeast Asia contribute 40% of the BC loading over the southeastern margin of the TP. The SBDART model showed that a DRE of +4.6 ± 2.4 W m^{-2} for the total $PM_{2.5}$ BC, of which +2.5 ± 1.8 W m^{-2} was from $BC_{biomass}$ and +2.1 ± 0.9 W m^{-2} from BC_{fossil}. The results of this study provide useful information concerning the sources of BC over an atmospheric transport channel to the southeastern TP, and they highlight the importance of the cross-border transport of biomass burning emissions from Southeast Asia on the region during the pre-monsoon.

删除了: regions
删除了: 9
删除了: T
删除了: the
删除了: is a
删除了: T
删除了: mass
删除了: explored
删除了: and the direct radiative forcing
删除了: the black carbon (
删除了:)
删除了: combustion
删除了: in the
删除了:
删除了: Tibetan Plateau
删除了: The observed mean BC concentration was 0.7 ± 0.5 μg m^{-3} during the campaign. Based on the optical source apportionment using multi-wavelength absorption and chemical species, the obtained absorption Ångström exponents (AAEs) and BC mass absorption cross section (MAC) at wavelength of 880 nm were
删除了: and
删除了: and
删除了: , respectively
删除了: Using these source-specific AAEs and BC MACs, the improved aethalometer model estimated
删除了: source
删除了: (BC_{fossil} and $BC_{biomass}$, respectively)
删除了: The diurnal cycle in $BC_{biomass}$ was driven by BC regional ...
删除了: (
删除了:)
设置了格式: 下标
删除了: from the
删除了: can
删除了: at the sampling site
删除了: The southeast of Gaomeigu was the most likely contributi ...
删除了: Santa Barbara DISORT Atmospheric Radiative Transfer (
删除了:)
删除了: estimated
删除了: a cooling effect of -3.0 ± 1.5 W m^{-2} at the Earth's surface ...
删除了: ,
删除了: comprising 73% of that caused by $PM_{2.5}$. The average ...
删除了: The average heating rate caused by BC was 0.13 ± 0.07 K ...

Data availability. All data described in this study are available upon request from the corresponding authors.

Supplement. The supplement related to this article is available online.

Author contributions. QW and JC designed the study. WR conducted the field measurements. LX provided the results of WRF-Chem model. YZ and TZ performed the chemical analysis of filters. HL and QW wrote the article. All the authors reviewed and commented on the paper.

Competing interests. The authors declare that they have no conflict of interest.

Acknowledgments. This work was supported by the National Natural Science Foundation of China (41877391), the Second Tibetan Plateau Scientific Expedition and Research Program (STEP) (2019QZKK0602), and the Youth Innovation Promotion Association of the Chinese Academy of Sciences (2019402).

References

Alfaro, S. C.: Iron oxides and light absorption by pure desert dust: An experimental study, J. Geophys. Res.-Atmos., 109, 10.1029/2003jd004374, 2004.

Bond, T. C., and Bergstrom, R. W.: Light absorption by carbonaceous particles: An investigative review, Aerosol. Sci. Tech., 40, 27-67, 10.1080/02786820500421521, 2006.

Bond, T. C., Doherty, S. J., Fahey, D. W., Forster, P. M., Berntsen, T., DeAngelo, B. J., Flanner, M. G., Ghan, S., Kärcher, B., Koch, D., Kinne, S., Kondo, Y., Quinn, P. K., Sarofim, M. C., Schultz, M. G., Schulz, M., Venkataraman, C., Zhang, H., Zhang, S., Bellouin, N., Guttikunda, S. K., Hopke, P. K., Jacobson, M. Z., Kaiser, J. W., Klimont, Z., Lohmann, U., Schwarz, J. P., Shindell, D., Storelvmo, T., Warren, S. G., and Zender, C. S.: Bounding the role of black carbon in the climate system: A scientific assessment, J. Geophys. Res.-Atmos., 118, 5380-5552, 10.1002/jgrd.50171, 2013.

Cao, J. J., Zhu, C. S., Tie, X. X., Geng, F. H., Xu, H. M., Ho, S. S. H., Wang, G. H., Han, Y. M., and Ho, K. F.: Characteristics and sources of carbonaceous aerosols from Shanghai, China, Atmos. Chem. Phys., 13, 803-817, 10.5194/acp-13-803-2013, 2013.

Cao J., Tie X., Xu B., Zhao, Z., Zhu, C., Li, G., and Liu, S.: Measuring and modelling black carbon (BC) contamination in the SE Tibetan Plateau, J. Atmos. Chem., 10.1007/s10874-011-9202-5, 2010.

Carrico, C. M., Gomez, S. L., Dubey, M. K., and Aiken, A. C.: Low hygroscopicity of ambient fresh carbonaceous aerosols from pyrotechnics smoke, Atmos. Environ., 178, 101-108, 10.1016/j.atmosenv.2018.01.024, 2018.

Chan, C. Y., Wong, K. H., Li, Y. S., Chan, Y., and Zhang, X. D.: The effects of Southeast Asia fire activities on tropospheric ozone, trace gases and aerosols at a remote site over the Tibetan Plateau of Southwest China, Tellus B., 58B, 310-318, 10.1111/j.1600-0889.2006.00187.x, 2017

Chen, B., Bai, Z., Cui, X., Chen, J., Andersson, A., and Gustafsson, O.: Light absorption enhancement of black carbon from urban haze in Northern China winter, Environ. Pollut., 221, 418-426, 10.1016/j.envpol.2016.12.004, 2017.

Cheng, M.-D., and Lin, C.-J.: Receptor modeling for smoke of 1998 biomass burning in Central America, J. Geophys. Res.-Atmos., 106, 22871-22886, 10.1029/2001jd900024, 2001.

Cheng, Y., Li, S., Leithead, A.: Chemical characteristics and origins of nitrogen-containing organic compounds in $PM_{2.5}$ aerosols in the lower fraser valley, Environ. Sci. Technol., 40, 5846-5852, 10.1021/es0603857, 2006.

Coen, M.C, Weingartner, E., Apituley, A., Ceburnis, D., Fierz-Schmidhauser, R., Flentje, H., Henzing, B., Jennings, S., Moerman, M., Petzold, A., Schmid, O., and Baltensperger, U.: Minimizing light absorption measurement artifacts of the Aethalometer: Evaluation of five correction algorithms, Atmos. Meas. Tech., 3, 457-474, 10.5194/amt-3-457-2010, 2009.

Cong, Z., Kang, S., Kawamura, K., Liu, B., Wan, X., Wang, Z., Gao, S., and Fu, P.: Carbonaceous aerosols on the south edge of the Tibetan Plateau: concentrations, seasonality and sources, Atmos. Chem. Phys., 10.5194/acp-15-1573-2015, 2015.

Draxler, R., and Hess, G.: An overview of the HYSPLIT_4 modelling system for trajectories, Aust. Meteorol. Mag., 47, 1998.

Drinovec, L., Močnik, G., Zotter, P., Prévôt, A. S. H., Ruckstuhl, C., Coz, E., Rupakheti, M., Sciare, J., Müller, T., Wiedensohler, A., and Hansen, A. D. A.: The "dual-spot" Aethalometer: an improved measurement of aerosol black carbon with real-time loading compensation, Atmos. Meas. Tech., 8, 1965-1979, 10.5194/amt-8-1965-2015, 2015.

Dubovik, O., Holben, B., Eck, T. F., Smirnov, A., Kaufman, Y. J., King, M. D., Tanré, D., and Slutsker, I.: Variability of absorption and optical properties of key aerosol types observed in worldwide locations, J. Atmos. Sci., 59, 590-608, 10.1175/1520-0469(2002)059<0590:VOAAOP>2.0.CO;2, 2002.

Dumka, U. C., Kaskaoutis, D. G., Tiwari, S., Safai, P. D., Attri, S. D., Soni, V. K., Singh, N., and Mihalopoulos, N.: Assessment of biomass burning and fossil fuel contribution to black carbon concentrations in Delhi during winter, Atmos. Environ., 194, 93-109, 10.1016/j.atmosenv.2018.09.033, 2018.

Forello, A. C., Bernardoni, V., Calzolai, G., Lucarelli, F., Massabo, D., Nava, S., Pileci, R. E., Prati, P., Valentini, S., Valli, G., and Vecchi, R.: Exploiting multi-wavelength aerosol absorption coefficients in a multi-time resolution source apportionment study to retrieve source-dependent absorption parameters, Atmos. Chem. Phys., 19, 11235-11252, 10.5194/acp-19-11235-2019, 2019.

Guo, H., Ding, A. J., So, K. L., Ayoko, G., Li, Y. S., and Hung, W. T.: Receptor modeling of source apportionment of Hong Kong aerosols and the implication of urban and regional contribution, Atmos. Environ., 43, 1159-1169, doi.org/10.1016/j.atmosenv.2008.04.046, 2009.

Hao, Y., Gao, C., Deng, S., Yuan, M., Song, W., Lu, Z., and Qiu, Z.: Chemical characterisation of $PM_{2.5}$ emitted from motor vehicles powered by diesel, gasoline, natural gas and methanol fuel, Sci. Total Environ., 674, 128-139, 10.1016/j.scitotenv.2019.03.410, 2019.

Han, H., Wu, Y., Liu, J., Zhao, T. Zhuang, B., Li, Y., Chen, H., Zhu, Y., Liu, H., Wang, Q., Wang, T., Xie, M., and Li, M.: Impacts of atmospheric transport and biomass burning on the interannual variation in black carbon aerosols over the Tibetan Plateau, Atmos. Chem. Phys., 10.5194/acp-2020-299, 2020.

Harrison, R. M., Beddows, D. C. S., Hu, L., and Yin, J.: Comparison of methods for evaluation of wood smoke and estimation of UK ambient concentrations, Atmos. Chem. Phys., 12, 8271-8283, 10.5194/acp-12-8271-2012, 2012.

Healy, R. M., Sofowote, U., Su, Y., Debosz, J., Noble, M., Jeong, C. H., Wang, J. M., Hilker, N., Evans, G. J., Doerksen, G., Jones, K., and Munoz, A.: Ambient measurements and source apportionment of fossil fuel and biomass burning black carbon in Ontario, Atmos. Environ., 161, 34-47, 10.1016/j.atmosenv.2017.04.034, 2017.

Helin, A., Niemi, J. V., Virkkula, A., Pirjola, L., Teinilä, K., Backman, J., Aurela, M., Saarikoski, S., Rönkkö, T., Asmi, E., and Timonen, H.: Characteristics and source apportionment of black carbon in the Helsinki metropolitan area, Finland, Atmos. Environ., 190, 87-98, 10.1016/j.atmosenv.2018.07.022, 2018.

Hess, M., Koepke, P., and Schult, I.: Optical properties of aerosols and clouds: The software package OPAC, American Meteorological Society, 79, 831-844, 10.1175/1520-0477(1998)079<0831:Opoaac>2.0.Co;2, 1998.

Hsu, C.-Y., Chiang, H.-C., Lin, S.-L., Chen, M.-J., Lin, T.-Y., and Chen, Y.-C.: Elemental characterization and source apportionment of PM 10 and PM 2.5 in the western coastal area of central Taiwan, Sci. Total Environ., 541, 1139-1150, 10.1016/j.scitotenv.2015.09.122, 2016.

Hua S., Liu, Y., Luo Run., Shao, T., and Zhu, Q.: Inconsistent aerosol indirect effects on water clouds and ice clouds over the Tibetan Plateau, Int. J. Climatol., 1-17, doi:10.1002/joc.6430, 2019.

Kant, Y., Shaik,D., S., Mitra, D., Chandola, H., Babu, S. S., and Chauhan, P., Black carbon aerosol quantification over north-west himalayas: Seasonal heterogeneity, source apportionment and radiative forcing, Environ. Pollut., 10.1016/j.envpol.2019.113446, 2019.

Kim, E., and Hopke, P. K.: Source characterization of ambient fine particles at multiple sites in the Seattle area, Atmos. Environ., 42, 6047-6056, 10.1016/j.atmosenv.2008.03.032, 2008.

Kirchstetter, T. W., Novakov, T., and Hobbs, P. V.: Evidence that the spectral dependence of light absorption by aerosols is affected by organic carbon, J. Geophys. Res.-Atmos., 109, 10.1029/2004jd004999, 2004.

Koch, D., Schulz, M., Kinne, S., McNaughton, C., Spackman, J. R., Balkanski, Y.,Bauer, S., Berntsen, T., Bond, T. C., Boucher, O., Chin, M., Clarke, A., De Luca, N., Dentener, F., Diehl, T., Dubovik, O., Easter, R., Fahey, D. W., Feichter, J., Fillmore, D., Freitag, S., Ghan, S., Ginoux, P., Gong, S., Horowitz, L., Iversen, T., Kirkevåg, A., Klimont, Z., Kondo, Y., Krol, M., Liu, X., Miller, R., Montanaro, V., Moteki, N., Myhre, G., Penner, J. E., Perlwitz, J., Pitari, G., Reddy, S., Sahu, L., Sakamoto, H., Schuster, G., Schwarz, J. P., Seland, Ø., Stier, P., Takegawa, N., Takemura, T., Textor, C., van Aardenne, J. A., and Zhao, Y.: Evaluation of black carbon estimations in global aerosol models, Atmos. Chem. Phys., 10.5194/acp-9-9001-2009,2009.

Kurokawa, J., Ohara, T., Morikawa, T., Hanayama, S., Janssens-Maenhout, G., Fukui, T., Kawashima, K., and Akimoto, H.: Emissions of air pollutants and greenhouse gases over Asian regions during 2000–2008: Regional Emission inventory in ASia (REAS) version 2, Atmos. Chem. Phys., 13, 11019-11058, 10.5194/acp-13-11019-2013, 2013.

Lack, D. A., and Cappa, C. D.: Impact of brown and clear carbon on light absorption enhancement, single scatter albedo and absorption wavelength dependence of black carbon, Atmos. Chem. Phys., 10, 4207-4220, 10.5194/acp-10-4207-2010, 2010.

Li, C., Bosch, C., Kang, S., Andersson, A. Chen., P. Zhang, Q., Cong., Z. Chen, B., and Gustafsson., Ö.: Sources of black carbon to the Himalayan–Tibetan Plateau glaciers, Nat. Commun., 7, 12574, https://doi.org/10.1038/ncomms12574, 2016.

Li, M., Zhang, Q., Kurokawa, J.I., Woo, J.H., He, K., Lu, Z., Ohara, T., Song, Y., Streets, D.G., Carmichael, G.R., Cheng, Y., Hong, C., Huo, H., Jiang, X., Kang, S., Liu, F., Su, H., Zheng, B., 2017. MIX: a mosaic Asian anthropogenic emission inventory under the international collaboration framework of the MICS-Asia and HTAP. Atmos. Chem. Phys. 17, 935-963, 10.5194/acp-17-935-2017

Liu, Y, Sato, Y., Jia, R, Xie, J, Huang, J, and Nakajima, T.: Modeling study on the transport of summer dust and anthropogenic aerosols over the Tibetan Plateau, Atmos. Chem. Phys., 15, 12581–12594, 10.5194/acp-15-12581-2015, 2015.

Liu, T.-Y.: Spatial structure convergence of China's transportation system, Research in Transportation Economics, 78, 10.1016/j.retrec.2019.100768, 2019a.

Liu Y., Q. Zhu, J. Huang, S. Hua, and Jia, Rui.: Impact of dust-polluted convective clouds over the Tibetan Plateau on downstream precipitation, Atmos. Environ., doi.org/10.1016/j.atmosenv.2019.04.001, 2019b.

Liu Y., Zhu, Q., Hua, S., Alam, K., and Cheng, Y.,: Tibetan Plateau driven impact of Taklimakan dust on northern rainfall, Atmos. Environ. 10.1016/j.atmosenv.2020.117583, 2020a.

Liu Y., Y. Li, J. Huang, Q. Zhu and S. Wang.:Attribution of the Tibetan Plateau to Northern Drought, Natl. Sci. Rev., doi:10.1093/nsr/nwz191, 2020b.

Liu, Y., Yan, C., and Zhang M.: Source apportionment of black carbon during winter in Beijing, Sci. Total Environ., 618, 531-541, 10.1016/j.scitotenv.2017.11.053, 2018.

Luo M., Y. Liu, Q. Zhu, Y. Tang and K. Alam.: Role and mechanisms of black carbon affecting water vapor transport to Tibet, Remote Sens., 10.3390/rs12020231, 2020.

Lough, G. C., Schauer, J. J., Park, J. S., Shafer, M. M., Weinstein, J. P.: Emissions of metals associated with motor vehicle roadways, Environ. Sci. Technol., 39, 826-836, 10.1021/es048715f, 2005.

Ma, Y., Huang, C., Jabbour, H., Zheng, Z., Wang, Y., Jiang, Y., Zhu, W., Ge, X., Collier, S., and Zheng, J.: Mixing state and light absorption enhancement of black carbon aerosols in summertime Nanjing, China, Atmos. Environ., 222, 10.1016/j.atmosenv.2019.117141, 2020.

Madala, S., Satyanarayana, A. N. V, Rao, T. N.: Performance evaluation of PBL and cumulus parameterization schemes of WRF ARW model in simulating severe thunderstorm events over Gadanki MST radar facility — Case study, Atmos. Res., 10.1016/j.atmosres.2013.12.017, 2014.

Ming, J., Xiao, C., Cachier, H., Qin, D., Qin, X., Li, Z., and Pu, J.: Black Carbon (BC) in the snow of glaciers in west China and its potential effects on albedos, Atmos. Res., 92, 114-123, 10.1016/j.atmosres.2008.09.007, 2009.

Niu H., Kang S., Zhang Y., Distribution of light-absorbing impurities in snow of glacier on Mt. Yulong, southeastern Tibetan Plateau, Atmospheric Research, 10.1016/j.atmosres.2017.07.004, 2017.

Panicker, A. S., Pandithurai, G., Safai, P. D., Dipu, S., and Lee, D.-I.: On the contribution of black carbon to the composite aerosol radiative forcing over an urban environment, Atmos. Environ., 44, 3066-3070, 10.1016/j.atmosenv.2010.04.047, 2010.

设置了格式: 字体: (中文) +中文正文 (宋体), (中文) 中文(中国)

带格式的: 缩进: 左侧: 0 厘米, 悬挂缩进: 2 字符, 首行缩进: -2 字符

Polissar, A. V., Hopke, P. K., Paatero, P., Kaufmann, Y. J., Hall, D. K., Bodhaine, B. A., Dutton, E. G., and Harris, J. M.: The aerosol at Barrow, Alaska: long-term trends and source locations, Atmos. Environ., 33, 2441-2458, 10.1016/S1352-2310(98)00423-3, 1999.

Polissar, A. V., Hopke, P. K., and Harris, J. M.: Source regions for atmospheric aerosol measured at Barrow, Alaska, Environ. Sci. Technol., 35, 4214-4226, 10.1021/es0107529, 2001.

Rai, M., Mahapatra, P. S., Gul, C., Kayastha, R. B., Panday, A. K., and Puppala, S. P.: Aerosol radiative forcing estimation over a remote high-altitude location (~4900 masl) near Yala Glacier, Nepal, Aerosol Air. Qual. Res., 19, 1872-1891, 10.4209/aaqr.2018.09.0342, 2019.

Ramachandran, S., and Kedia, S.: Black carbon aerosols over an urban region: Radiative forcing and climate impact, J. Geophys. Res., 115, 10.1029/2009jd013560, 2010.

Rajesh, T. A., and Ramachandran, S.: Black carbon aerosols over urban and high altitude remote regions: Characteristics and radiative implications, Atmos. Environ., 194, 110-122, 10.1016/j.atmosenv.2018.09.023, 2018.

Ricchiazzi, P., and Yang, S. J. B. o. t. A. M. S.: SBDART: A research and teaching software tool for plane-parallel radiative transfer in the earth's atmosphere, 79, 2101-2114, 10.1175/1520-0477(1998)0792.0.CO;2 1998.

Sandradewi, J., Prévôt, A. S. H., Weingartner, E., Schmidhauser, R., Gysel, M., and Baltensperger, U.: A study of wood burning and traffic aerosols in an Alpine valley using a multi-wavelength Aethalometer, Atmos. Environ., 42, 101-112, 10.1016/j.atmosenv.2007.09.034, 2008.

Song, Y., Zhang, Y., Xie, S., Zeng, L., Zheng, M., Salmon, L. G., Shao, M., and Slanina, S.: Source apportionment of PM2.5 in Beijing by positive matrix factorization, Atmos. Environ., 40, 1526-1537, 10.1016/j.atmosenv.2005.10.039, 2006.

Sun, J., Zhi, G., Hitzenberger, R., Chen, Y., Tian, C., Zhang, Y., Feng, Y., Cheng, M., Zhang, Y., Cai, J., Chen, F., Qiu, Y., Jiang, Z., Li, J., Zhang, G., and Mo, Y.: Emission factors and light absorption properties of brown carbon from household coal combustion in China, Atmos. Chem. Phys., 17, 4769-4780, 10.5194/acp-17-4769-2017, 2017.

Tian, J., Wang, Q., Ni, H., Wang, M., Zhou, Y., Han, Y., Shen, Z., Pongpiachan, S., Zhang, N., Zhao, Z., Zhang, Q., Zhang, Y., Long, X., and Cao, J.: Emission characteristics of primary brown carbon

删除了:

设置了格式: 字体: (中文) +中文正文 (宋体), (中文) 中文(中国)

absorption from biomass and coal burning: Development of an optical emission inventory for China, J. Geophys. Res.-Atmos., 10.1029/2018jd029352, 2019.

Urban, R. C., Lima-Souza, M., Caetano-Silva, L., Queiroz, M. E. C., Nogueira, R. F. P., Allen, A. G., Cardoso, A. A., Held, G., and Campos, M. L. A. M.: Use of levoglucosan, potassium, and water-soluble organic carbon to characterize the origins of biomass-burning aerosols, Atmos. Environ., 61, 562-569, 10.1016/j.atmosenv.2012.07.082, 2012.

Valenzuela, A., Olmo, F. J., Lyamani, H., Antón, M., Titos, G., Cazorla, A., and Alados-Arboledas, L.: Aerosol scattering and absorption Angström exponents as indicators of dust and dust-free days over Granada (Spain), Atmos. Res., 154, 1-13, 10.1016/j.atmosres.2014.10.015, 2015.

Vignati, E., Karl, M., Krol, M., Wilson, J., Stier, P., and Cavalli, F.: Sources of uncertainties in modelling black carbon at the global scale, Atmos. Chem. Phys., 10.5194/acp-10-2595-2010,2010.

Wang, Q., Cao, J., Han, Y., Tian, J., Zhu, C., Zhang, Y., Zhang, N., Shen, Z., Ni, H., Zhao, S., and Wu, J.: Sources and physicochemical characteristics of black carbon aerosol from the southeastern Tibetan Plateau: internal mixing enhances light absorption, Atmos. Chem. Phys., 18, 4639-4656, 10.5194/acp-18-4639-2018, 2018.

Wang, Q., Han, Y., Ye, J., Liu, S., Pongpiachan, S., Zhang, N., Han, Y., Tian, J., Wu, C., Long, X., Zhang, Q., Zhang, W., Zhao, Z., and Cao, J.: High contribution of secondary brown carbon to aerosol light absorption in the southeastern margin of Tibetan Plateau, Geophys. Res. Lett., 46, 4962-4970, 10.1029/2019gl082731, 2019a.

Wang, Q., Ye, J., Wang, Y., Zhang, T., Ran, W., Wu, Y., Tian, J. Li, L., Zhou. Y., Ho., S., Dang, B., Zhang, Q., Zhang, R., Chen, Y., Zhu, C., and Cao, J.: Wintertime optical properties of primary and secondary brown carbon at a regional site in the North China Plain, Environ. Sci. Technol., 53, 12389-12397, 10.1021/acs.est.9b03406, 2019b.

Wang, Q. Y., Huang, R. J., Cao, J. J., Tie, X. X., Ni, H. Y., Zhou, Y. Q., Han, Y. M., Hu, T. F., Zhu, C. S., Feng, T., Li, N., and Li, J. D.: Black carbon aerosol in winter northeastern Qinghai–Tibetan Plateau, China: the source, mixing state and optical property, Atmos. Chem. Phys., 15, 13059-13069, 10.5194/acp-15-13059-2015, 2015.

Xing, L., Li, G., Pongpiachan, S., Wang, Q., Han, Y., Cao, J., Tipmanee, D., Palakun, J., Aukkaravittayapun, S., Surapipith, V., and Poshyachinda, S.: Quantifying the contributions of local emissions and regional transport to elemental carbon in Thailand, Environ Pollut, 262, 114272, 10.1016/j.envpol.2020.114272, 2020.

Xia, X , Zong, X , Cong, Z , Chen, H., Kang, S., and Wang, P.: Baseline continental aerosol over the central Tibetan plateau and a case study of aerosol transport from South Asia, Atmos. Environ., 10.1016/j.atmosenv.2011.07.067, 2011.

Xu, J. Z., Zhang, Q., Wang, Z. B., Yu, G. M., Ge, X. L., and Qin, X.: Chemical composition and size distribution of summertime PM2.5 at a high altitude remote location in the northeast of the Qinghai–Xizang (Tibet) Plateau: insights into aerosol sources and processing in free troposphere, Atmos. Chem. Phys., 15, 5069-5081, 10.5194/acp-15-5069-2015, 2015.

Yang, K., Wu, H., Qin, J., Lin, C., Tang, W., and Chen, Y.: Recent climate changes over the Tibetan Plateau and their impacts on energy and water cycle: A review, Global Planet. Change, 112, 79-91, 10.1016/j.gloplacha.2013.12.001, 2014.

Zhang, R., Wang, H., Qian, Y., Rasch, P. J., Easter, R. C., Ma, P. L., Singh, B., Huang, J., and Fu, Q.: Quantifying sources, transport, deposition, and radiative forcing of black carbon over the Himalayas and Tibetan Plateau, Atmos. Chem. Phys., 15, 6205-6223, 10.5194/acp-15-6205-2015, 2015.

Zhang, Y., Li M., Cheng, Y., Geng, G., Hong, C., Li, H., Li, X., Tong D. Wu, N, Zhang, X., Zheng, Y., Bo, Y., Su, H., and Zhang, Q.: Modeling the aging process of black carbon during atmospheric transport using a new approach: a case study in Beijing, Atmos. Chem. Phys., doi.org/10.5194/acp-19-9663-2019, 2019.

Zhao, Z., Cao, J., Chow, J. C., Watson, J. G., Chen, A. L. W., Wang, X., Wang, Q., Tian, J., Shen, Z., Zhu, C., Liu, S., Tao, J., Ye, Z., Zhang, T., Zhou, J., and Tian, R.: Multi-wavelength light absorption of black and brown carbon at a high-altitude site on the Southeastern margin of the Tibetan Plateau, China, Atmos. Environ., 212, 54-64, 10.1016/j.atmosenv.2019.05.035, 2019.

Zhu, C. S., Cao, J. J., Hu, T. F., Shen, Z. X., Tie, X. X., Huang, H., Wang, Q. Y., Huang, R. J., Zhao, Z. Z., Mocnik, G., and Hansen, A. D. A.: Spectral dependence of aerosol light absorption at an urban

and a remote site over the Tibetan Plateau, Sci Total Environ, 590-591, 14-21, 10.1016/j.scitotenv.2017.03.057, 2017.

Zotter, P., Herich, H., Gysel, M., El-Haddad, I., Zhang, Y. L., Mocnik, G., Huglin, C., Baltensperger, U., Szidat, S., and Prevot, A. H.: Evaluation of the absorption angstrom ngstrom exponents for traffic and wood burning in the Aethalometer-based source apportionment using radiocarbon measurements of ambient aerosol, Atmos. Chem. Phys, 17, 4229-4249, 10.5194/acp-17-4229-2017, 2017.

Table 1 Derived Ångström absorption exponents (AAE), Mass absorption coefficients (MAC) and percent source contribution of black carbon (BC) from difference sources

	AAE	MAC (m^2 g^{-1})	Mass concentration (μg m^{-3})	Contribution ratio
$BC_{biomass}$	1.7	10.4	0.4 ± 0.3	57%
$BC_{traffic}$	0.8	9.1	---	---
BC_{coal}	1.1	15.5	---	---
BC_{fossil}	0.9	12.3	0.3 ± 0.2	43%

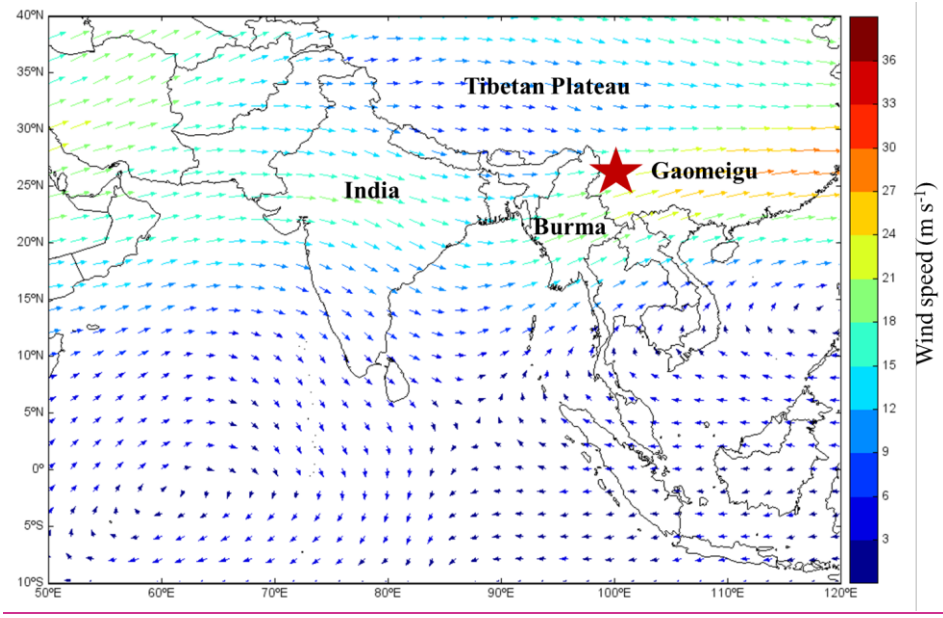

Figure 1. Location of the Gaomeigu sampling site on the southeastern margin of Tibetan Plateau and prevailing wind speeds and directions during sampling period

带格式的: 左

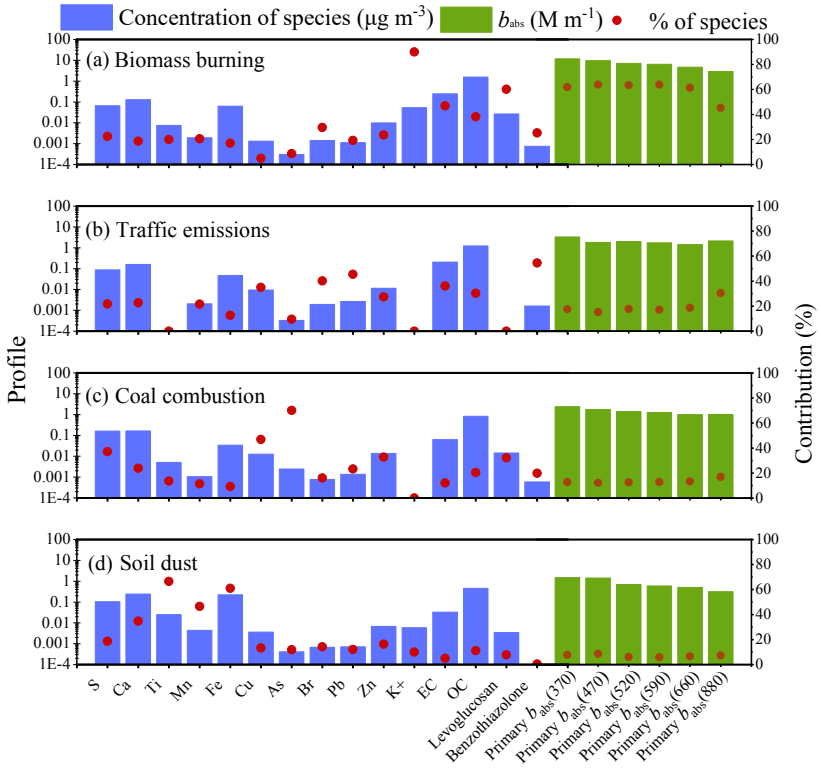

Figure 2. Four aerosol light absorption sources identified by a positive matrix factorization (PMF) model. Concentration (μg m^{-3}) of the chemical species in each source are colored by purple. Primary b_{abs} (λ) at six wavelengths (λ = 370, 470, 520, 590, 660, or 880nm) in each source (M m^{-1}) are colored by green.

删除了: 1

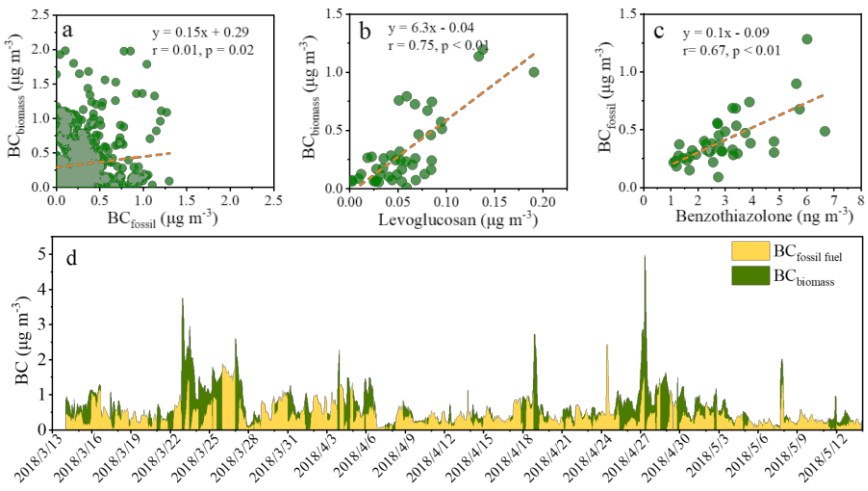

Figure 3. Scatter plots of (a) biomass burning black carbon ($BC_{biomass}$) versus fossil fuel combustion BC (BC_{fossil}), (b) $BC_{biomass}$ versus levoglucosan, and (c) BC_{fossil} versus benzothiazolone. $BC_{biomass}$ and BC_{fossil} repreent black carbon aerosol contributed by biomass burning and fossil fuel sources, respectively. (d)Time series of hourly-averaged mass concentrations of black carbon (BC) aerosol from biomass bunirng ($BC_{biomass}$) and fossil fuel sources (BC_{fossil}).

删除了：

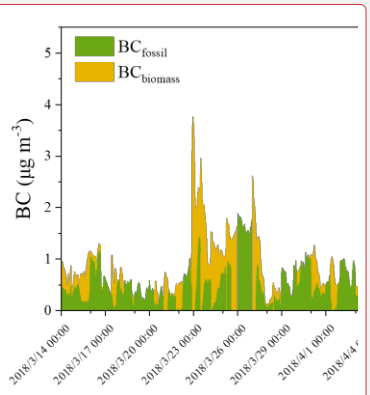

删除了：**Figure 2.** Time series of hourly averaged mass concentrations of black carbon (BC) aerosol from biomass bunirng ($BC_{biomass}$) and fossil fuel sources (BC_{fossil}) during the campaign.

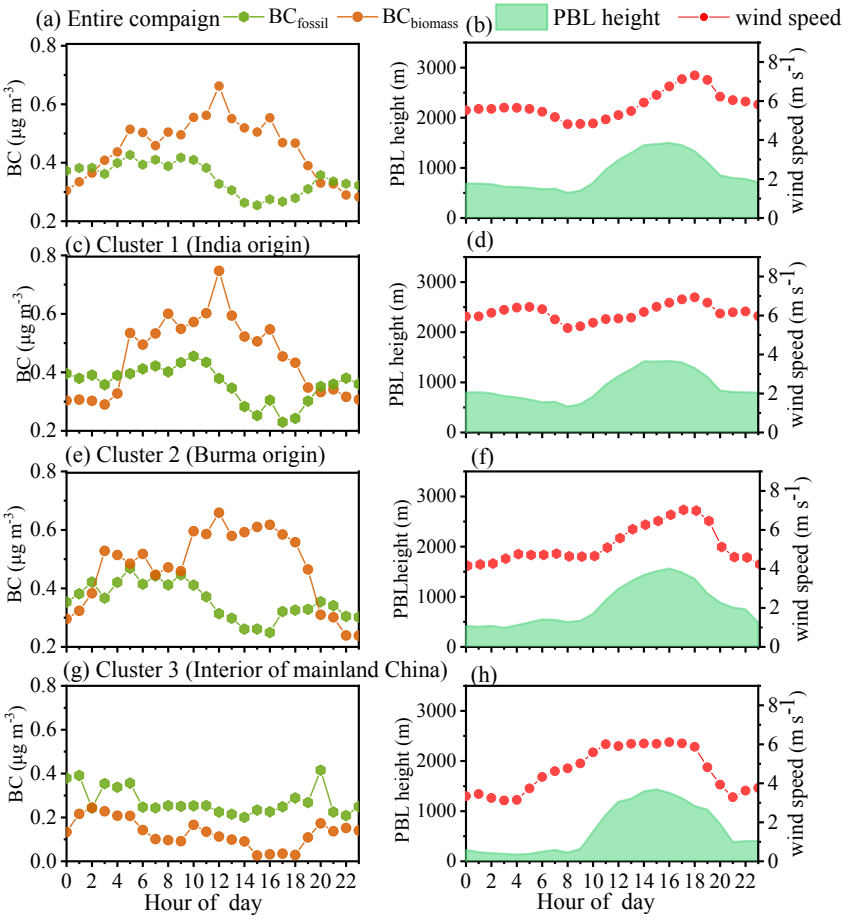

Figure 4. (Left panel) Diurnal variations of hourly averaged black carbon (BC) aerosol from biomass burning ($BC_{biomass}$) and fossil fuel sources (BC_{fossil}). (Right panel) wind speed and planetary boundary layer (PBL) height during the entire campaign and different air-mass directions as determined by air-mass trajectory clusters 1-3.

删除了: 3
删除了: l
删除了: as well as
删除了: r

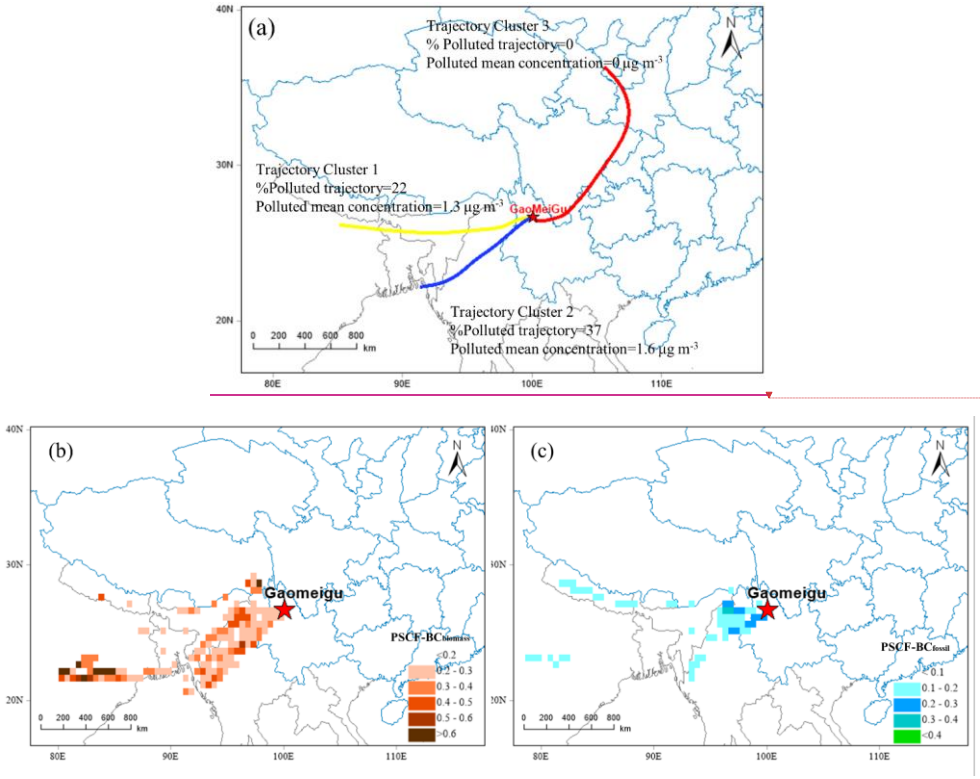

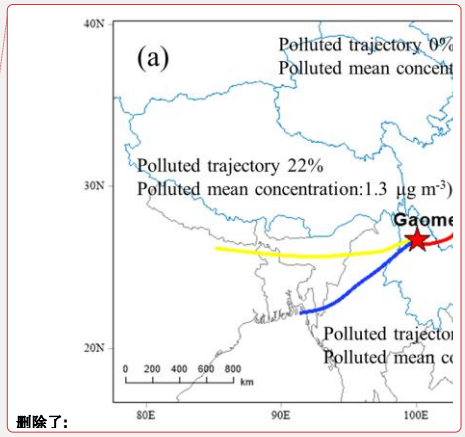

删除了：

Figure 5. Maps of (a) the mean trajectory clusters and the potential source contribution function for black carbon (BC) aerosol from (b) biomass burning ($BC_{biomass}$) and (c) fossil fuel sources (BC_{fossil}).

删除了：4

删除了：during the campaign

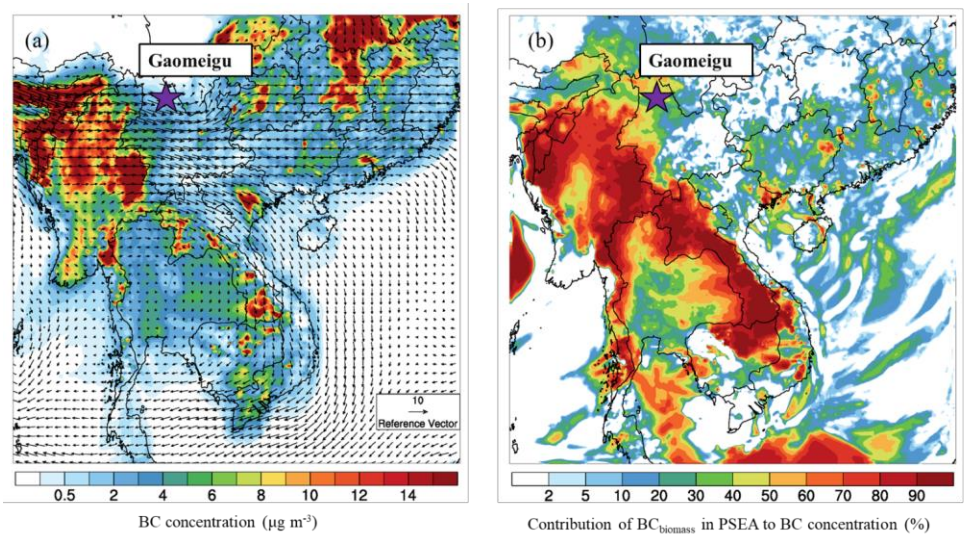

Figure 6. (a) Spatial distributions of simulated black carbon (BC) mass concentrations in Southeast Asia and (b) the percent mass contribution of biomass-burning BC ($BC_{biomass}$) in peninsular Southeast Asia (PSEA). The simulated surface winds are overlaid on (a).

删除了: 5

删除了: were

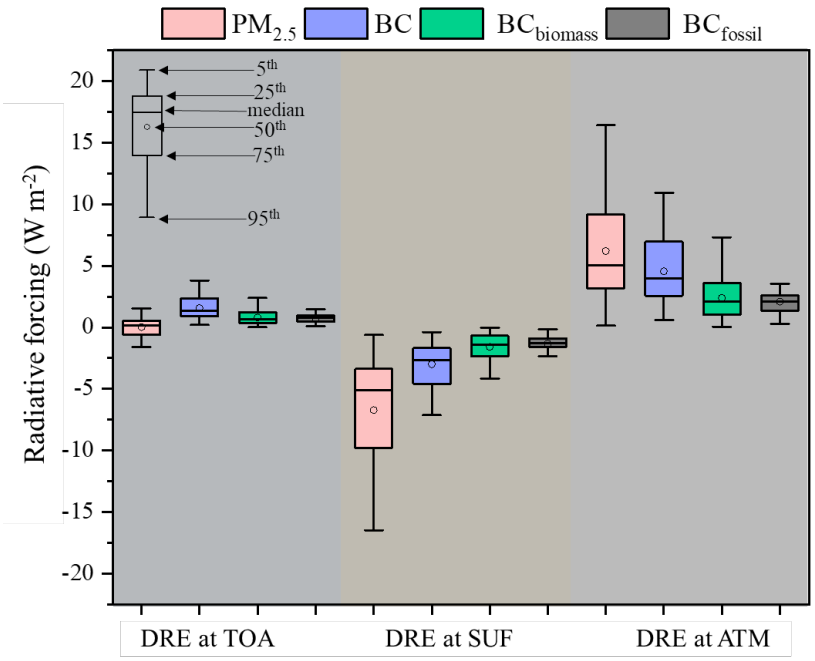

Figure 7. The average direct radiative forcing (DRF) of black carbon (BC) aerosol and $PM_{2.5}$ at the Earth's surface (SUF), the top of atmsphere (TOA), and in the atmosphere (ATM= TOA – SUF). The $BC_{biomass}$ and BC_{fossil} represent BC contributed by biomass burning and fossil fuel sources, respectively.

带格式的: 居中, 缩进: 左侧: 0 厘米, 首行缩进: 0 字符

删除了:

删除了: 6

删除了: F